JAERI-Research
2003-020

RE-EVALUATION OF NEUTRON NUCLEAR DATA FOR ^{129}I AND ^{143}Nd

September 2003

Tsuneo NAKAGAWA and Akira HASEGAWA

日本原子力研究所
Japan Atomic Energy Research Institute

本レポートは、日本原子力研究所が不定期に公刊している研究報告書です。
入手の問合わせは、日本原子力研究所研究情報部研究情報課（〒319-1195 茨城県那珂郡東海村）あて、お申し越し下さい。なお、このほかに財団法人原子力弘済会資料センター（〒319-1195 茨城県那珂郡東海村日本原子力研究所内）で複写による実費頒布を行っております。

This report is issued irregularly.
Inquiries about availability of the reports should be addressed to Research Information Division, Department of Intellectual Resources, Japan Atomic Energy Research Institute, Tokai-mura, Naka-gun, Ibaraki-ken 〒319-1195, Japan.

編集兼発行　日本原子力研究所

JAERI－Research 2003－020

Re-evaluation of Neutron Nuclear Data for ^{129}I and ^{143}Nd

Tsuneo NAKAGAWA and Akira HASEGAWA

Department of Nuclear Energy System
Tokai Research Establishment
Japan Atomic Energy Research Institute
Tokai-mura, Naka-gun, Ibaraki-ken

(Received August 1, 2003)

The evaluated nuclear data for ^{129}I and ^{143}Nd stored in JENDL-3.3 were investigated comparing with other evaluated data and experimental data. New experimental data were available especially for the capture cross sections of both nuclides. The parameters used in theoretical calculations were modified so as to reproduce those experimental data. The statistical model calculation was performed using the revised parameters. The resonance parameters were also revised so that the cross sections measured in the thermal energy region were reproduced well. The present results were compiled in the ENDF-6 format.

Keywords: Nuclear Data, Evaluation, Iodine-129, Neodymium-143, Cross Sections, Resonance Parameters, Thermal Cross Sections

^{129}I および ^{143}Nd に対する中性子核データの再評価

日本原子力研究所東海研究所エネルギーシステム研究部
中川　庸雄・長谷川　明

(2003年8月1日受理)

JENDL-3.3 に格納されている ^{129}I と ^{143}Nd の核データを、他の評価済みデータや実験データと比較して検討した。特に、中性子捕獲断面積に対しては新しい実験データがどちらの核種にもある。理論計算に使用するパラメータをこれらの実験データを再現するように調整し、統計模型による計算をおこなった。また、分離共鳴パラメータを修正し、熱中性子エネルギーにおける実験データを良く再現するようにした。評価の結果をENDF-6 フォーマットで編集した。

東海研究所：〒319-1195 茨城県那珂郡東海村白方白根 2–4

Contents

1. Introduction 1
2. Iodine-129 1
2.1 Resolved Resonance Parameters 1
2.2 Unresolved Resonance Parameters 3
2.3 Cross Sections in the Smooth Region 3
2.3.1 Optical Model Parameters and Statistical Model Calculation with CASTHY Code 3
2.3.2 Neutron Capture Cross Section 4
2.3.3 Inelastic Scattering Cross Sections 5
2.3.4 Threshold Reaction Cross Sections 5
2.3.5 Elastic Scattering Cross Section 6
2.4 Other Data 6
3. Neodymium-143 6
3.1 Resolved Resonance Parameters 6
3.2 Unresolved Resonance Parameters 8
3.3 Cross Sections in the Smooth Region 8
3.3.1 Optical Model Parameters and Statistical Model Calculation with CASTHY Code 8
3.3.2 Neutron Capture Cross Section 9
3.3.3 Inelastic Scattering Cross Sections 10
3.3.4 (n,α) Reaction Cross Section 10
3.3.5 Threshold Reaction Cross Sections 11
3.3.6 Elastic Scattering Cross Section 11
3.4 Other Data 12
4. Conclusions 12
Acknowledgements 13
References 13

目　　次

1. はじめに 1
2. ヨウ素 129 1
2.1 分離共鳴パラメータ 1
2.2 非分離共鳴パラメータ 3
2.3 連続領域の断面積 3
2.3.1 光学模型パラメータと CASTHY による統計模型計算 3
2.3.2 中性子捕獲断面積 4
2.3.3 非弾性散乱断面積 5
2.3.4 しきい反応断面積 5
2.3.5 弾性散乱断面積 6
2.4 その他のデータ 6
3. ネオジム 143 6
3.1 分離共鳴パラメータ 6
3.2 非分離共鳴パラメータ 8
3.3 連続領域の断面積 8
3.3.1 光学模型パラメータと CASTHY による統計模型計算 8
3.3.2 中性子捕獲断面積 9
3.3.3 非弾性散乱断面積 10
3.3.4 (n,α)反応断面積 10
3.3.5 しきい反応断面積 11
3.3.6 弾性散乱断面積 11
3.4 その他のデータ 12
4. 結　論 12
謝　辞 13
参考文献 13

1. Introduction

Nowadays accurate nuclear data are required to the fission product (FP) nuclides. The data stored in JENDL-3.3 [Sh02] were those evaluated by Kawai et al. [Ka92] for JENDL-3.1 and revised [Ka01] for JENDL-3.2. After the re-evaluation work for JENDL-3.2, several sets of new experimental data have been available.

In the present work, the data of ^{129}I and ^{143}Nd of JENDL-3.3 were investigated comparing with recent experimental data, and new evaluation work was performed. The nuclide of ^{129}I has a long life-time of 1.57×10^{7} years. Therefore this nuclide is one of the important long-lived FP nuclides. The nuclide of ^{143}Nd is a stable one. However, its FP yield is very large; for example, cumulative yield from ^{235}U thermal neutron-induced fission is 5.9%. Furthermore the capture cross sections of Nd isotopes are also important for s-process calculation in astrophysics.

The present work for ^{129}I and ^{143}Nd will be described in Chapter 2 and 3, respectively.

2. Iodine-129

2.1 Resolved Resonance Parameters

The data for JENDL-3.3 were evaluated on the basis of the resonance parameters analyzed by Macklin [Ma83]. Macklin measured the capture cross section using ORELA, and reported the capture areas in the neutron energy region below 3.16 keV. In the previous evaluation, the neutron widths were determined adopting his data and assuming the capture width of 120 meV.

After the evaluation for JENDL-3.3, Noguere et al. [No01] reported preliminary resonance parameters for 24 resonances below 1 keV which were obtained by analyzing the transmission data measured at GELINA of IRMM with the R-matrix code REFIT.

In the present evaluation, we modified the resonance parameters of JENDL-3.3 considering partly the preliminary results of Noguere et al. They reported the neutron and capture widths of three resonances at 41.4, 72.1 and 96.3 eV. Especially the resonance at 41.4 eV has not been measured by previous authors. The parameters of these three resonances were adopted in the present evaluation.

Noguere et al. determined the parameters of a negative resonance at –9.55 eV so as to reproduce the thermal capture cross section of 30.3±1.2 b measured by Nakamura et al. [Na96]

However, they failed to reproduce the capture resonance integral of 33.8±1.4 b [Na96] which was larger than 28.3 b calculated from the parameters of Noguere et al. We found that it was most suitable to remove the negative resonance and to give a 1/v-type background cross section to the capture cross section. The contribution to the capture cross section from the positive resonance is only 0.2 b at 0.0253 eV. To compensate the cross section of 30 b, we gave the 1/v-type background. Then we could obtain the resonance integral of 33.9 b which was in very good agreement with the data of Nakamura et al.

The effective scattering radius of 5.48 fm was adopted in JENDL-3.3, which was estimated from systematics shown by Mughabghab et al. [Mu81] (Fig.1 of [Mu81]). However, in the present evaluation, we did not adopt this radius, because the negative resonance at –9.55 eV was removed and this value of scattering radius could not reproduce the total cross section in the thermal region. We adopted the scattering radius of 6.0 fm to reproduce the total cross section of 35±4 b measured by Block et al. [Bl60].

The upper boundary of resolved resonance region was set to 3.391 keV, and the multi-level Breit-Wigner formula was selected for the cross-section calculation formula. This choice is the same as JENDL-3.3.

The average level spacing and s-wave neutron strength function obtained from the resolved resonance parameters were 28 eV and 0.71×10^{-4}, respectively. Figure 2.1 shows cumulative numbers of resonances and Fig. 2.2 sum of reduced neutron widths.

The cross sections at 0.0253 eV and resonance integrals are compared in Tables 2.1 and 2.2, respectively. The present result of capture cross section is about 10% larger than JENDL-3.3, and in good agreement with Nakamura et al. The total cross section is also consistent with the data of Block et al. [Bl60]. The resonance integral of the present evaluation is the same as Nakamura et al., and larger than JENDL-3.3.

The total cross sections below 500 eV are shown in Fig. 2.3. The present evaluation gives almost the same cross section as JENDL-3.3 and ENDF/B-VI below about 10 eV. They are in agreement with the data of Block et al. CENDL-3 adopted the resonance parameters of JENDL-3.2 which was the same as JENDL-3.3.

The capture cross section of present evaluation is compared with experimental data and other evaluations in Fig. 2.4. Since the present evaluation gave the 1/v-type background to the capture cross section, the shape of capture cross section is very different from previous evaluations in particular above about 1 eV. Kobayashi et al. measured the capture cross section using the 46-MeV LINAC and TOF method in the energy range from 0.005 eV to 40 keV. Their data are still preliminary. Since they normalized their data to ENDF/B-VI (27.04 b) at 0.0253 eV,

their cross sections are systematically smaller than the present evaluation. However the cross-section shape is in good agreement with the present one.

2.2 Unresolved Resonance Parameters

In the energy range from 3.391 to 100 keV, unresolved resonance parameters were given. The code ASREP [Ki99] was used to determine the parameters to reproduce the average cross sections in this energy region. As will be described in the next section, the average capture cross sections were calculated with the optical and statistical model code CASTHY [Ig91] and in good agreement with experimental data. The total cross section calculated with CASTHY code at 100 keV was also considered in the parameter fitting.

The initial parameters were average level spacing (D_0) of 28 eV, scattering radius (R) of 6.0 fm, s-wave neutron strength function (S_0) of 0.71×10^{-4}, p-wave one (S_1) of 1.7×10^{-4}, d-wave one (S_2) of 9.0×10^{-4} and average capture width (Γ_γ) of 80 meV. D_0, R and S_0 were adopted from the resolved resonance parameters of present evaluation. Concerning the average capture width, if we used the value of 120 meV adopted for the resolved resonances, a very large level spacing was obtained. The 120 meV seemed to be too large. Therefore, the average capture width of 80 meV was assumed in the unresolved resonance region. Others were calculated with the optical model using the CASTHY code.

In the fitting procedure, the average level spacing was adjusted at each neutron energy to reproduce the capture cross section calculated with CASTHY code, and the scattering radius to the total cross section at 100 keV. Then, the level spacing of 27 to 28 eV and the radius of 5.64 fm were obtained. Figure 2.5 compares the cross sections calculated from the unresolved resonance parameters with those to be reproduced. The results are quite satisfactory.

2.3 Cross Sections in the Smooth Region

2.3.1 Optical Model Parameters and Statistical Model Calculation with CASTHY Code

No experimental data are available for the total cross section of ^{129}I above the resonance region. Assuming that the total cross section of ^{127}I is almost the same as that of ^{129}I, the data of JENDL-3.3 is compared with experimental data [Ma65, Go67, Ta68, An70, An71, Fo71] of ^{127}I total cross section reported after 1960, in Fig. 2.6. It is seen that the JENDL-3.3 is too small around 100 keV, and is slightly shifted in shape to the high energy side in the MeV region. CENDL-3 reproduces better these experimental data. The cross section below 100 keV has a

strange shape. In the previous evaluation, since the average level spacing was fitted to the experimental data of capture cross section at each neutron energy, the fluctuation of capture cross section was reflected to the total cross section.

In the present work, the optical potential parameters were determined so as to reproduce the ^{127}I total cross sections measured by Foster and Glasgow [Fo71] in the MeV region and Tabony and Seth [Ta68] from 30 to 600 keV. Potential parameters for ^{127}I were determined by using the TOTAL code [IgP1]. Igarasi potential [Ig73] was adopted as an initial set of parameters. Results are listed in Table 2.3 together with the previous potential parameters. The total cross sections for ^{127}I and ^{129}I calculated from the new parameters are shown in Fig.2.6 comparing with the experimental data. Since the parameters have mass-number dependence, the present calculations for both isotopes are different from each other.

The evaluated total cross sections of ^{129}I are shown in Fig. 2.7. The present results below 100 keV are the cross sections calculated from new unresolved resonance parameters. Below several keV, average cross sections are shown because this region is the resolved resonance region.

In the statistical model calculation with CASTHY code, level density parameters, gamma-ray strength function and level scheme listed in Table 2.4 were used. The level density parameters were determined from the average resonance level spacing and staircase plot of excited levels. The staircase plots of ^{129}I and ^{130}I are shown in Figs. 2.8 and 2.9. The level density parameters of ^{130}I were largely improved. The threshold reaction cross sections such as (n,2n), (n,3n) were calculated with EGNASH2 code [Ya90, Yo92]. The direct inelastic scattering cross section was calculated with DWUCKY code [Ya88, KuP1] Sum of the threshold reaction cross sections and direct inelastic scattering cross sections were considered as a competing reaction cross section in the statistical model calculation with CASTHY code.

2.3.2 Neutron Capture Cross Section

In the previous evaluation for JENDL-3.3, the capture cross section was calculated with CASTHY code normalizing the gamma-ray strength function to the experimental data of Macklin [Ma83]. Recently Kobayashi et al. [Ko02] and Matsumoto et al. [Ma02] have performed new experiments. Their results are still preliminary.

The preliminary experimental data of Kobayashi et al. and Matsumoto et al. are in agreement with each other and smaller than the previous Macklin's data. In the present calculations, the gamma-ray strength function was normalized to the data of Matsumoto et al.; 183 mb at 64 keV. The obtained gamma-ray strength function is 0.00289 as listed in Table 2.4.

In the MeV region, direct/semi-direct capture cross section was calculated with a simple equation proposed by Benzi and Reffo [Be69], and normalized to 1 mb at 14 MeV. Nakano et al. [Na97] and Murata et al. [Mu97] reported the capture cross sections of 13±2 mb at 14.6 MeV and 32±3 mb at 14.8 MeV, respectively. They measured them by using DT neutron source at OKTAVIAN of the Osaka University. However, we did not adopt their results because they reported that their results contained contributions from low energy neutrons.

The capture cross section in the energy range from 1 keV to 20 MeV is shown in Fig. 2.10. The present calculation reproduces well the data of Matsumoto et al. and those of Kobayashi et al., and smaller than the data of Macklin and JENDL-3.3.

2.3.3 Inelastic Scattering Cross Sections

The level scheme in Table 2.4 was determined from the recent data of ENSDF [Te96]. Levels up to 1.483 MeV were taken into consideration in the present evaluation. The spin and parity of 1.1967 MeV level was adopted from RIPL-2 [Ia03].

The direct inelastic scattering was calculated with DWBA code DWUCKY [Ya88, KuP1] for the levels marked with "*" in Table 2.4. The deformation parameters of β_2 for those levels were estimated in DWUCKY code from an average value for even-even nuclides of 0.152 which were obtained from neighboring nuclides [Ra01]. The modified parameters of Walter-Guss optical potential given in DWUCKY code were applied. The compound inelastic was calculated with CASTHY code.

The total inelastic scattering cross section is compared with other evaluations in Fig. 2.11.

2.3.4 Threshold Reaction Cross Sections

EGNASH2 code [Ya90] was used to calculate the cross sections of (n,n'), (n,2n), (n,3n), (n,nα), (n,np), (n,nd), (n,γ), (n,p), (n,d), (n,t), (n,^{3}He) and (n,α) reactions. The information on excited levels and level density parameters were needed for the calculation. The level information was adopted from ENSDF [En02], and level density parameters were determined from staircase plots of excited levels. The level density parameters are given in Table 2.5. We could not determine the level density parameter for ^{126}Sb because the number of excited levels was not enough. For ^{126}Sb the systematics in EGNASH2 was used.

For the calculation of transmission coefficients, the default optical model parameters of EGNASH2 were used: modified Walter and Guss potential [Ya90, Wa85] for neutrons, Perey and Walter-Guss potential [Wa85] for protons, Lemos potential modified by Arthur and Young [Ar80] for α particles, and Lohr and Haeberli potential [Lo74] for deuterons.

Figure 2.12 shows the (n,2n) and (n,3n) reaction cross sections. There are experimental data for the (n,2n) reaction cross sections around 14 MeV. The data of JENDL-3.3 was normalized to the old data [Ku73] which is larger than recent experiments [Na97, Mu97]. The f2 parameters of EGNASH2 input was adjusted to reproduce these recent data. We adopted the f2 of 0.5 which is much smaller than the value of 1.3 to 1.6 recommended in the manual [Yo92].

Plompen et al. [Pl01] reported results of recent measurements of ^{129}I(n,2n) cross section made at GEEL. Their data in a figure are about 1 to 0.5 b in the energy range from 16 to 20 MeV. Those data were not considered in the present work because their data were preliminary, and we found difficulty to reproduce such small (n,2n) cross sections.

Figures 2.13 to 2.19 show the (n,p), (n,α), (n,np), (n,nα), (n,d), (n,t) and (n,nd) reaction cross sections. No experimental data are available for these reactions. ENDF/B-VI did not give the data for them. There are quite large discrepancies among the evaluated data.

2.3.5 Elastic Scattering Cross Section

The elastic scattering cross section was calculated as the total cross section minus a sum of partial cross sections. The result is the same as the CASTHY calculation. Figure 2.20 compares the present result with other evaluations.

2.4 Other Data

The angular distributions of elastically scattered neutrons adopted in the present work are the results of CASTHY calculation. For those of inelastic scattering, a sum of CASTHY calculation and DWUCKY calculation was adopted. For the other reactions, isotropic distributions in the laboratory system were assumed.

The energy distributions were calculated with EGNASH2 code. Interpolation scheme of 22 (unit-base interpolation) [Mc01] was adopted for all the reactions.

3. Neodymium-143

3.1 Resolved Resonance Parameters

In the previous evaluation, the resolved resonance parameters were determined on the basis of resonance parameters reported by Tellier [Te71], Musgrove et al. [Mu77] and Rohr et al.

[Ro71] The parameters of a negative resonance at –6 eV were adjusted so as to reproduce the thermal cross sections recommended by Mughabghab et al. [Mu81]

The comparison of thermal cross sections is made in Table 3.1. Several measurements have been reported on the thermal capture cross sections. Mughabghab [Mu81, Mu03] recommended the capture cross section of 325±10 b based on these experiments. Evaluated data reproduce well this recommendation. For the elastic scattering, experimental data are scarce. Evaluations are based on the data of Vertebnyj et al. [Ve74] We found two experimental data [Ha58, Ve74] for the total cross section. Evaluated data are smaller than these two data.

The total and capture cross sections below 500 eV are shown in Figs. 3.1 and 3.2. The data of Vertebnyj et al. [Ve74] are available below 10 eV for both cross sections. All the evaluations are smaller than the experimental data above 1 eV especially for the capture cross section.

No recent analyses of resonance parameters have been reported after the previous evaluation and any problems have not been found to the resonance parameters of JENDL-3.3. Therefore we modified only the parameters of a negative resonance to improve the cross sections in the low energy region.

Finally the parameters of the resonance at –6 eV were replaced with the following values:

$E_r = -10$ eV, $\Gamma_n = 0.52$ eV, $\Gamma_\gamma = 0.111$ eV.

The thermal cross sections calculated after this modification are listed in Table 3.1 as the present results. The thermal cross sections of present evaluation are about 2% larger than JENDL-3.3, and in good agreement with the experimental data. Cross section curves are shown in Figs. 3.3 and 3.4.

The resonance integrals are given in Table 3.2. The present value is 10% larger than JENDL-3.3 and the recommendation of Mughabghab [Mu03].

The upper boundary of the resolved resonance region was set to be 5 keV. The multi-level Breit-Wigner formula was selected as the resonance formula. The effective scattering radius of 5.6 fm (same as JENDL-3.3) was adopted.

Figure 3.5 shows the total cross section in the energy range from 100 eV to 1 keV and from 1 to 3 keV. Experimental data shown in the figures are those of Tellier [Te71] measured by using LINAC and a sample in the purity of 83.2 %. Since the isotopes of ^{142}Nd and ^{144}Nd were also included in the sample, their resonances are seen also in the figures.

3.2 Unresolved Resonance Parameters

The unresolved resonance parameters were given in the energy range from 5 to 100 keV. The parameters were determined using ASREP code to reproduce the capture cross section in this energy range and the total cross section at 100 keV calculated with CASTHY code.

The initial parameters were selected as follows:

Average level spacing (D_0)	45 eV
Scattering radius (R)	5.6 fm
s-wave neutron strength function (S_0)	3.2×10^{-4}
p-wave neutron strength function (S_1)	0.8×10^{-4}
d-wave neutron strength function (S_2)	3.0×10^{-4}
Average capture width (Γ_γ)	80 meV

The scattering radius is the same value as the resolved resonance region. S_2 was calculated with the optical model. Other parameters are recommendations of Mughabghab et al. [Mu81] The cross sections calculated from the obtained unresolved resonance parameters are compared with the cross sections calculated with CASTHY code in Fig. 3.6. The capture cross sections are perfectly reproduced with the present parameters. The total cross sections at several tens keV are not reproduced because we adopted s-wave neutron strength function smaller than CASTHY calculation; for example, the CASTHY calculation is 3.9×10^{-4} at 10 keV.

3.3 Cross Sections in the Smooth region

3.3.1 Optical Model Parameters and Statistical Model Calculation with CASTHY Code

The optical model parameters used in the previous evaluation for JENDL-3.3 have not reproduced well the total cross section. Figure 3.7 shows measured total cross sections and JENDL-3.3. The experimental data for ^{143}Nd are only those of Djumin et al. [Dj73] at 14.2 MeV and Wisshak et al. [Wi97a] from 12.5 to 175 keV. Assuming that the total cross section is not so strongly dependent on mass numbers, we also depicted the total cross section of ^{144}Nd [Sh80] and natural Nd [Fo71, Po83] in Fig. 3.7. The data of JENDL-3.3 are not in agreement with the experimental data above about 7 MeV, and smaller than Wisshak et al. in the keV region.

In Fig. 3.7, the total cross section calculated from Konig-Delaroche potential [Ko03] is also shown. This set of optical potential predicts well the total cross section in the MeV region, but smaller than JENDL-3.3 in the hundred keV region.

In the present parameter search, we used the TOTAL code [IgP1], and Igarasi potential

[Ig73] as an initial set. Obtained optical model parameters are given in Table 3.3. The total cross section calculated from the new potential is shown in Fig. 3.7 with a solid line. Figure 3.8 extends the comparison to the other evaluated data and the energy region down to 1 keV. It is seen the present optical model parameters reproduce well the experimental data.

The new set of optical model parameters was used for the calculation of total, elastic and inelastic scattering, and capture cross sections. In the statistical model calculation with CASTHY code, level density parameters, gamma-ray strength function and level scheme shown in Table 3.4 were used. The level density parameters for Gilbert-Cameron's formula were determined from the average resonance level spacing and staircase plot of excited levels. The threshold reaction cross sections such as (n,2n), (n,3n) were calculated with EGNASH2 code [Ya90, Yo92]. The direct inelastic scattering was calculated with DWUCKY code [Ya88, KuP1] Sum of the threshold reaction cross sections and direct inelastic scattering cross sections were considered as a competing reaction cross section in the CASTHY code.

3.3.2 Neutron Capture Cross Section

Wisshak et al. [Wi97a, Wi98] and Veerapaspong et al. [Ve99] reported new experimental data, in the energy range from 6 to 220 keV and from 22 to 550 keV, respectively, which are in good agreement with each other. In the previous evaluation for JENDL-3.3, the gamma-ray strength function was normalized to the data of Nakajima et al. [Na78] However, the recent data are smaller than Nakajima et al. by 10 to 30 %.

In the present evaluation, the CASTHY calculation was normalized to 147 mb at 65 keV so as to reproduce the data of Veerapaspong et al. Then the gamma-ray strength function was decreased from 2.15×10^{-3} of JENDL-3.3 to 1.65×10^{-3}. The result of CASTHY calculation is shown in Fig. 3.9 with a dashed line. Unfortunately the energy dependence was not the same as the experimental data. We modified them by multiplying an energy dependent factor; 1.2 below 6 keV and 1.15 above 500 keV. The result is a solid line in Fig. 3.9.

The direct/semi-direct capture cross section in the MeV region was calculated from the equation of Benzi and Reffo [Be69], and added to the modified CASTHY calculation.

The present evaluation is compared with other evaluations and experimental data [Mu78, Na78, Bo85, Wi97a, Ve99] in Fig. 3.10. In the energy range from 5 to 100 keV, the present evaluation is calculated from the unresolved resonance parameters.

Maxwellian-averaged capture cross section is important for astprophysics. Wisshak et al. [Wi97b] obtained the Maxwellian-averaged cross section from the capture cross sections measured at 3 to 225 keV using a Van der Graaf accelerator and a 4π BaF_2 detector. Figure 3.11

shows their results together with the average cross sections obtained from the present evaluation and JENDL-3.3. The recommendation of Bao et al. [Ba00] is also plotted. The data of Bao et al. were based on the data of Wisshak et al. It is seen that the present evaluation is in good agreement with the data of Wisshak et al. Table 3.5 shows the average capture cross sections at thermal energies of kT = 10 and 30 keV. The present evaluation is slightly smaller than Wisshak et al. at 10 keV.

3.3.3 Inelastic Scattering Cross Sections

The level scheme of ^{143}Nd for calculation of the inelastic scattering cross sections was adopted from the evaluation of Tuli [Tu01] stored in ENSDF. We adopted 30 levels listed in Table 3.4 including the ground state because the statistical model code CASTHY has a limitation of 30 to the levels considered. Four levels at 1.55884, 1.690, 1.900 and 1.920 MeV were ignored because of no information on their spin and parity.

The direct inelastic cross sections were calculated with DWUCKY code [Ya88, KuP1] for the levels marked with asterisk in Table 3.4. The deformation parameters β_2 for these levels were estimated in DWUCKY code using average β_2 of 0.11 obtained from the recommendations by Raman et al. [Ra01]

The total inelastic scattering cross section is shown in Fig. 3.12 comparing with other evaluations. No experimental data are available.

3.3.4 (n,α) Reaction Cross Section

The (n,α) reaction cross section is shown in Fig. 3.13. The Q-value of this reaction is positive, and experimental data exist at thermal neutron energy. In the previous evaluation, the (n,α) cross section was calculated from resonance formula assuming an average α width of 3.48×10^{-6} eV so that the cross section at 0.0253 eV was 0.0174 b recommended by Mughabghab et al. [Mu81] After the calculation average cross sections in suitable energy meshes were stored in JENDL-3.3.

In the present work, the α widths measured by Antonov et al. [An84] were adopted. They measured the (n,α) cross section by means of TOF, and analyzed 10 resonance peaks. For other resonances, a constant width of 4×10^{-6} eV was applied. This value was obtained so as to reproduce the thermal cross section of 20 mb which was a weighted average of the data of Cheifetz et al. [Ch62] and Asghar and Emsallem [As78] The cross sections calculated from the resonance parameters were averaged in the suitable energy meshes. Above about 1.6 keV, the experimental data of Andzheevskiy et al. [An81] and Popov et al. [Po80] are available. A

smooth curve was drown by eye-guide to these experimental data, and to connected to the cross sections above 4 MeV calculated with EGNASH2 code and normalized to 4 mb at 14 MeV [Fo86].

The (n,α) cross section of JENDL-3.3 was calculated with PEGASUS code [Na99] above 100 keV. The shape below several MeV was not suitable. The data of CENDL-3 has incorrect interpolation scheme below 5 keV. ENDF/B-VI and JEFF-3.0 ignored the experimental data.

3.3.5 Threshold Reaction Cross Sections

EGNASH2 code [Ya90] was used to calculate the cross sections of (n,n'), (n,2n), (n,3n), (n,nα), (n,np), (n,nd), (n,γ), (n,p), (n,d), (n,t), (n,^{3}He) and (n,α) reactions. The results were adopted to the present evaluation except for the inelastic scattering and capture cross sections.

The level schemes of related nuclides were taken from ENSDF as of December 2002. The maximum discrete level was determined from staircase plots of the excited levels. Default values of *a* parameters given in EGNASH2 code were adopted to whole nuclides.

For the calculation of transmission coefficients, the default optical model parameters of EGNASH2 were used: modified Walter and Guss potential [Ya90, Wa85] for neutrons, Perey and Walter-Guss potential [Wa85] for protons, Lemos potential modified by Arthur and Young [Ar80] for α particles, and Lohr and Haeberli potential [Lo74] for deuterons.

A constant for calculation of matrix elements for two-body interaction f2 of 0.5 was used. If we use the values of 1.3 to 1.6, the calculated (n,p) cross section were much larger than the experimental data [Co59]. Smaller f2 was preferable in order to reproduce the (n,p) cross section of Coleman et al. [Co59]

Figure 3.14 shows the (n,2n) and (n,3n) reaction cross sections.

Figure 3.15 is the (n,p) cross section. As described above, the data of Coleman et al. [Co59] exists at 14.5 MeV. Evaluated data including the present one, excluding ENDF/B-VI, are in good agreement with the experimental data.

Figures 3.16 to 3.21 show the (n,nα), (n,np), (n,nd), (n,d), (n,t) and (n,^{3}He) reaction cross sections. No experimental data are available for these reactions. For the (n,nα) cross sections, ENDF/B-VI and CENDL-3 give small cross sections in the low energy region while the present evaluation assumed them to be 0.0 below 4 MeV.

3.3.6 Elastic Scattering Cross Section

The elastic scattering cross section was calculated as the total cross section minus a sum of partial cross sections. The result is the same as the CASTHY calculation. Figure 3.22

compares the present result with other evaluations.

3.4 Other Data

The angular distributions of elastically scattered neutrons calculated with CASTHY code were adopted. For those of inelastic scattering, sum of CASTHY and DWUCKY calculations was adopted. For the other reactions, isotropic distributions in the laboratory system were assumed.

The energy distributions were calculated with EGNASH2 code. Interpolation scheme of 22 [Mc01] was adopted for all the reactions.

4. Conclusions

The evaluated data of ^{129}I and ^{143}Nd stored in JENDL-3.3 were revised. For both nuclides, a part of resonance parameters and parameters for theoretical calculation were improved and new calculations were performed. These parameters were adjusted to reproduce the recent experimental data.

The cross sections in the low energy region were improved. The previous evaluation for ^{129}I and ^{143}Nd gave a negative resonance so as to reproduce thermal capture cross sections. However, the recent experimental data of ^{129}I capture cross section show a 1/v behavior below the first positive resonance. This means that a 1/v-type background cross section is preferable to a negative resonance. On the other hand, for ^{143}Nd we could reproduce the experimental data by changing parameters of the negative resonance.

In the smooth-cross section region, the optical model parameters were improved. The capture cross sections were revised to reproduce the recent experimental data. Threshold reaction cross sections were calculated with EGNASH2 code. The results were largely different from previous ones. We need experimental data for these threshold reactions in order to provide more accurate cross section data.

The present results were compiled in the ENDF-6 format.

Acknowledgements

The authors appreciate the support of Dr. Makoto Ishikawa, JNC, to the present work. They also thank Drs. Katsuhei Kobayashi, Kyoto University, and Tetsuro Matsumoto and Masayuki Igashira, Tokyo Institute of Technology, for providing us with their recent experimental data.

References

To the references whose experimental data were taken from EXFOR which is a database of experimental data, its entry number is also given.

[An70] Angeli I., Csikai J. and Hunyadi I.: *Acta Phys. Acad. Sci. Hung.*, **28**, 87 (1970), EXFOR 30113.

[An71] Angeli I., Csikai J., Nagy J.L., Scharbert T., Sztaricskai T. and Novak D.: *Acta Phys. Acad. Sci. Hung.*, **30**, 115 (1971), EXFOR 30141.

[An81] Andzheevski Yu., Vo Kim Tkhan', Vtyurin V.A., Korejvo A., Popov Yu.P. and Stehmpin'ski M.: INDC(CCP)-177/L, p.7 (1981), translation from *Yadernye Konstanty*, 1/40, 13 (1981), EXFOR 40667.

[An84] Antonov A., Gledenov Yu.M., Marinova S., Popov Yu.P. and Rigol H.: *Sov. J. Nucl. Phys.*, **39**, 501 (1984).

[Ar80] Arthur E.D. and Young P.G: "Evaluated Neutron-Induced Cross Sections for ^{54,56}Fe to 40 MeV," *LA*-8626-MS (1980).

[As78] Asghar M. and Emsallem A.: *Proc. 3rd Int. Symp. Neutron Capture Gamma Ray Spectroscopy and Related Topics*, BNL, USA, Sep. 18 – 22, 1978, p.549 (1978), EXFOR 21302.

[Ba00] Bao Z.Y., Beer H., Käppeler F., Voss F. and Wisshak K.: *At. Data Nucl. Data Tables*, **76**, 70 (2000).

[Be69] Benzi V. and Reffo G: *CCDN*-NW/10 (1969).

[Bl60] Block R.C., Slaughter G.G. and Harvey J.A.: *Nucl. Sci. Eng.*, **8**, 112 (1960), EXFOR 12024.

[Bo85] Bokhovko M.V. et al.: *Yadernye Konstanty*, 1985(3), 12 (1985), EXFOR 40938.

[Ca68] Cabell M.J. and Wilkins M.: *J. Inorg. Nucl. Chem.*, **30**, 897 (1968), EXFOR 21467.

[Ch62] Cheifetz E., Gilat J., Yavin A.I. and Cohen S.G.: *Phys. Lett.*, **7**, 289 (1962), EXFOR 31151.

[Co59] Coleman R.F. Hawker B.E., O'connor L.P., Perkin J.L.: *Proc. Phys. Soc.*, **73**, 215 (1959), EXFOR 21440.

[Cu57] Cummius J.D.: *AERE*-R/R-2333 (1957), EXFOR 21469.

[Dj73] Djumin A.N., Egorov A.I., Popova G.N. and Smolin V.A.: *Izv. Rossiiskoi Akademii Nauk, Ser. Fiz.*, **37**,1019 (1973), EXFOR 40302.

[En02] Bart M.R.: *Proc. International Conference on Nuclear Data for Science and Technology*, Juelich, May 13-17, 1991, p. 817 (1992).

[Fo71] Foster D.G.Jr. and Glasgow D.W.: *Phys. Rev.*, **C3**, 576 (1971), EXFOR 10047.

[Fo86] Forrest R.A.: "Systematics of Neutron-Induced Threshold Reactions with Charged Products at about 14.5 MeV," *AERE*-R 12419 (1986).

[Go67] Gorlov G.V., Lebedeva N.S. and Morozov V.M.: *Yadernaya Fizika*, **6**, 910 (1967), EXFOR 41311.

[Ha58] Hay H.J.: *J. Nucl. Energy*, **7**, 199 (1958)

[Ia03] IAEA, Nuclear Data Section: RIPL-2, Reference Input Parameter Library, http://ndsli01.iaea.org/RIPL-2/ (2003).

[IgP1] Igarasi S.: private communication.

[Ig73] Igarasi S., Kawai M., Nakagawa T., Suehiro T. and Murata T.: "Cross Sections of the Fission Product Nuclei," *JAERI* 1228, p.41 (1973). [in Japanese]

[Ig91] Igarasi S. and Fukahori T.: "Program CASTHY – Statistical Model Calculation for Neutron Cross Sections and Gamma Ray Spectrum –," *JAERI* 1321 (1991).

[Ka92] Kawai M., Iijima S., Nakagawa T., Nakajima Y., Sugi T., Watanabe T., Matsunobu H., Sasaki M. and Zukeran A.: *J. Nucl. Sci. Technol.*, **29**, 195 (1992).

[Ka01] Kasugai Y., Ikeda Y., Uno Y., Yamamoto H. and Kawade K.: "Activation Cross Section Measurement at Neutron Energy from 13.3 to 14.9 MeV using FNS Facility," *JAERI-Research* 2001-025 (2001).

[Ki99] Kikuchi Y., Nakagawa T. and Nakajima Y.: "ASREP: A Computer Program for Automatic Search of Unresolved Resonance Parameters," *JAERI-Data/Code* 99-025 (1999). [in Japanese]

[Ko02] Kobayashi K.: private communication (2002).

[Ko03] Koning A.J. and Delaroche J.P.: *Nucl. Phys.*, **A713**, 231 (2003).

[KuP1] Kunz P.D.: DWUCK, unpublished.

[Ku73] Kuhry J.G. and Bontems G.: *Radiochem. Radioanaly. Lett.*, **15**, 29 (1973),

EXFOR20365.

[Lo74] Lohr J.M. and Haeberli W.: *Nucl. Phys.*, **A232**, 381 (1974).

[Lu77] Lucas M., Hagemann R., Naudet R., Renson C. and Chevalier C.: *Proc. Meeting Technical Committee on Natural Fission Reactors*, Paris, France, Dec. 19-21, 1977, Vol. 1, p.431 (1978), EXFOR 21563.

[Ma65] Manero F.: *Nucl. Phys.*, **65**, 419 (1965), EXFOR 20209.

[Ma83] Macklin R.L.: *Nucl. Sci. Eng.*, **85**, 350 (1983).

[Ma02] Matsumoto T. and Igashira M.: private communication (2002).

[Mc01] (Ed.) McLane V.: "ENDF-102, Data Formats and Procedures for the Evaluated Nuclear Data File, ENDF-6," BNL-NCS-44945-01/04-Rev. (2001).

[Mu77] Musgrove A.R.de L., Allen B.J., Boldeman J.W. and Macklin R.L.: "Non-Statistical Effects in the Radiative Capture Cross Sections of the Neodymium Isotopes," *AREC*/E401 (1977).

[Mu78] Musgrove A.R. del L., Allen B.J., Boldeman J.W. and Macklin R.L.: *Proc. International Conference Neutron Physics and Nuclear Data for Reactors*, Harwell, UK, Sep. 25 – 29, 1978, p.449 (1978), EXFOR 30360.

[Mu81] Mughabghab S.F., Divadeenam M. and Holden N.E.: *Neutron Cross Sections, Vol. 1, Neutron Resonance Parameters and Thermal Cross Sections*, Part A., Z=1 – 60, Academic Press (1981).

[Mu97] Murata I., Nakano D. and Takahashi A.: *JAERI-Conf* 97-004, p.177 (1997).

[Mu03] Mughabghab S.F.: "Thermal Neutron Capture Cross Sections, Resonance Integrals and g-Factors," *INDC(NDS)*-440/PG+R (2003).

[Na78] Nakajima Y., Asami A., Kawarasaki Y., Furuta Y., Yamamoto T. and Kanda Y.: *Proc. International Conference Neutron Physics and Nuclear Data for Reactors*, Harwell, UK, Sep. 25 – 29, 1978, p.438 (1978).

[Na96] Nakamura S., Harada H., Katoh T. and Ogata Y.: *J. Nucl. Sci. Technol.*, **33**, 283 (1996).

[Na97] Nakano D., Murata I. and Takahashi A.: *JAERI-Conf* 97-005, p.216 (1997).

[Na99] Nakagawa T., Iijima S., Sugi T., Nishigori T.: "PEGASUS: A Preequilibrium and Multi-step Evaporation Code for Neutron Cross Section Calculation," *JAERI-Data/Code* 99-031 (1999).

[No01] Noguere G., Brusegan A., Lepretre A., Herault N., Galleano R. and Macavero E.: *Proc. International Conference on Nuclear Science and Technology*, Tsukuba, Japan, Oct. 7 – 12, 2001, Vol. 1, p.184 (2002).

[Pa63] Pattenden N.J.: *Nucl. Sci. Eng.*, **17**, 371 (1963), EXFOR 12025.

[Pl01] Plompen A.J.M., Smith D.L., Reimer P., Qaim S.M., Semkova V., Cserpák F., Avrigeanu V. and Sudár S.: *Proc. International Conference Nuclear Data for Science and Technology*, Tsukuba, Japan, Oct. 7 – 12, 2001, Vol. 1, p.192 (2002).

[Po52] Pomerance H.: *Phys. Rev.*, **88**, 412 (1952), EXFOR 11507.

[Po80] Popov Ju.P., Salackij V.I. and Khuu-Khen-Khuu G.: *Yadernaya Fizika*, **32**, 893 (1980), EXFOR 40611.

[Po83] Poenitz W.P. and Whalen J.F.: "Neutron Total Cross Section Measurements in the Energy Region from 47 keV to 20 MeV," *ANL-NDM*-80 (1983) EXFOR 12853.

[Ra01] Raman S., Nestor C.W. Jr. and Tikkanen P.: *At. Data Nucl. Data Tables*, **78**, 1 (2001).

[Ro58] Roy J.C. and Wuschke D.: *Can. J. Chem.*, **36**, 1424 (1958), EXFOR 12005.

[Ro71] Rohr G., Weigmann H. and Heske M.: *Proc. Third Conf. Neutron Cross Section and Technology,* Mar. 15 – 17, 1971, Knoxvile, Tennessee, USA, Vol.2, p.743 (1971).

[Sh80] Shamu R.E., Bernstein E.M. and Ramirez J.J.: *Phys. Rev.*, **C22**, 1857 (1980).

[Sh02] Shibata K., Kawano T., Nakagawa T., Iwamoto O., Katakura J., Fukahori T., Chiba S., Hasegawa A., Murata T., Matsunobu H., Ohsawa T., Nakajima Y., Yoshida T., Zukeran A., Kawai M., Baba M., Ishikawa M., Asami T., Watanabe T., Watanabe Y., Igashira M., Yamamuro N., Kitazawa H., Yamano N. and Takano H.: *J. Nucl. Sci. Technol.*, **39**, 1125 (2002).

[Ta60] Tattersall R.B., Rose H., Pattenden S.K. and Jowitt D.: *J. Nucl. Energy*, **A12**, 32 (1960), EXFOR 20638.

[Ta68] Tabony R.H. and Seth K.K.: *Ann. Phys.*, **46**, 401 (1968), EXFOR 11953.

[Te71] Tellier H.: *CEA*-N-1459 (1971), EXFOR 20118.

[Te96] Tendow Y.: *Nucl. Data Sheets*, **77**, 631 (1996).

[Tu01] Tuli J.K.: *Nucl. Data Sheets*, **94**, 605 (2001).

[Ve74] Vertebnyj V.P., Gnidak N.L. and Pavlenko E.A.: *YFI*-17, 37 (1974), EXFOR 40290.

[Ve99] Veerapaspong T., Igashira M., Mizuno S., Hori J. and Ohsaki T.: *J. Nucl. Sci. Technol.*, **36**, 855 (1999).

[Wa85] Walter R.L. and Guss P.P.: *Proc. International Conference Nuclear Data for Basic and Applied Science*, Santa Fe, USA, May 13 – 17, 1985, Vol. 2, 1079 (1985).

[Wi97a] Wisshak K., Voss F., Käppeler F., Guber K., Kazakov L. and Reffo G.: *KfK*-5967 (1997), EXFOR 22388.

[Wi97b] Wisshak K., Voss F., Käppeler F. and Kazakov L.: *Nucl. Phys.*, **A621**, 270c (1997).

[Wi98] Wisshak K., Voss F., Käppeler F., Kazakov L. and Reffo G: *Phys. Rev.*, **C57**, 391

(1998).

[Ya88] Yamamuro N.: "A Nuclear Cross Section Calculation System with Simplified Input-Format, Version I (SINCROS-I)," *JAERI-M* 88-140 (1988). [in Japanese]

[Ya90] Yamamuro N.: "A Nuclear Cross Section Calculation System with Simplified Input-Format, Version II (SINCROS-II)," *JAERI-M* 90-006 (1990).

[Yo92] Young P.G., Arthur E.D. and Chadwick M.B.: "Comprehensive Nuclear Model Calculations: Introduction to the Theory and Use of the GNASH Code," *LA*-12343-MS (1992).

Table 2.1 Thermal cross sections of ^{129}I

Unit: barns

Capture		
Present	30.00	
JENDL-3.3	27.00	
ENDF/B-VI	27.00	
JEFF-3.0	33.89	
CENDL-3	27.00	JENDL-3.2 was adopted.
Mughabghab et al. [Mu81]	27±2	recommendation
Roy et al. [Ro58]	26.7±2.0	Maxw. average
Pattenden [Pa63]	28±2	
Nakamura et al. [Na96]	30.3±1.2	
Elastic scattering		
Present	4.09	
JENDL-3.3	6.47	
ENDF/B-VI	4.54	
JEFF-3.0	8.54	
CENDL-3	6.47	JENDL-3.2 was adopted.
Total		
Present	34.09	
JENDL-3.3	33.47	
ENDF/B-VI	31.54	
JEFF-3.0	42.43	
CENDL-3	33.47	JENDL-3.2 was adopted.
Block et al. [Bl60]	35±4	Energy dependent exp.

Table 2.2 Resonance integrals of ^{129}I capture cross section

Unit: barns

Present	33.9	
JENDL-3.3	29.4	
ENDF/B-VI	35.8	
JEFF-3.0	30.6	
CENDL-3	29.4	JENDL-3.2 was adopted.
Mughabghab et al. [Mu81]	36±4	recommendation
Roy et al. [Ro58]	36.0±4.0	
Nakamura et al. [Na96]	33.8±1.4	

Table 2.3 Optical potential parameters for n+^{129}I reaction

For the previous evaluation

Potential shape: Derivative Woods-Saxon for surface-imaginary part

Depth (MeV)	Radius (fm)	Diffuseness (fm)
$V = 45.97 - 0.199 \times E$	6.481	0.62
$W_S = 6.502$	6.926	0.35
$V_{SO} = 7.0$	6.49	0.62

For the present evaluation

Potential shape: Derivative Woods-Saxon for surface-imaginary part

Depth (MeV)	Radius (fm)	Diffuseness (fm)
$V = 45.54 - 0.279 \times E$	$1.165 \times A^{1/3} + 0.6$	0.62
$W_I = 0.125 \times E - 0.0004 \times E^2$	$1.16 \times A^{1/3} + 0.6$	0.62
$W_S = 5.955$	$1.16 \times A^{1/3} + 1.1$	0.35
$V_{SO} = 7.0$	$1.16 \times A^{1/3} + 0.6$	0.62

A: mass number

Table 2.4 Parameters used in CASTHY calculation for ^{129}I

a) Level density parameters

Nuclide	a(1/MeV)	T(MeV)	spin-cutoff	Ex(MeV)	Pairing(MeV)
129I	17.20	0.62	15.46	5.762	1.20
130I	16.52	0.74	15.23	6.64	0.0

b) Gamma-ray strength function

2.89×10^{-3} adjusted to reproduce the capture cross section of about 183 mb at 64 keV

Table 2.4 Parameters used in CASTHY calculation for ^{129}I (continued)

c) Excited levels

No.	Energy(MeV)	Spin-parity		
0	0.0	7/2	+	
1	0.0278	5/2	+	*
2	0.27838	3/2	+	*
3	0.48735	5/2	+	
4	0.55962	1/2	+	
5	0.69589	7/2	+	*
6	0.72957	9/2	+	*
7	0.76876	7/2	+	
8	0.82992	3/2	+	
9	0.84482	7/2	+	
10	1.0474	3/2	+	
11	1.0502	7/2	+	
12	1.1117	5/2	+	
13	1.1967	1/2	−	taken from RIPL-2
14	1.2036	5/2	+	
15	1.2098	1/2	+	
16	1.2607	3/2	+	
17	1.2820	7/2	+	
18	1.2919	1/2	+	
19	1.4014	9/2	−	
20	1.4830	1/2	+	
	1.521			Above this energy, levels were assumed to be overlapping

Direct inelastic scattering was calculated to the levels with "*".

Table 2.5 Level density parameters used in EGNASH2 calculation

Nuclide	*a* parameter	comments
I-130	16.52	
I-129	17.20	
I-128	17.89	
I-127	17.17	
Te-129	20.15	
Te-128	18.00	
Sb-127	17.00	
Sb-126	--	systematics in egansh2 used
Sb-125	17.00	

Table 3.1 Thermal cross sections of ^{143}Nd

Unit: barns

Capture		
Present	332.12	
JENDL-3.3	325.01	
ENDF/B-VI	325.15	
JEFF-3.0	335.89	
CENDL-3	323.06	
Mughabghab et al. [Mu81]	325±10	recommendation
Pomerance [Po52]	292±8	Maxw. average
Cummius [Cu57]	236±13	Maxw. average
Hay [Ha58]	343±20	
Tattersall et al.[Ta60]	336±10	
Cabell et al. [Ca68]	318±13.6	
	316.1±13.5	Maxw. average
Vertebnyj et al. [Ve74]	338±8	
Lucas et al. [Lu77]	335	
Asghar et al. [As78]	325	Maxw. average
Elastic scattering		
Present	81.51	
JENDL-3.3	80.00	
ENDF/B-VI	80.10	
JEFF-3.0	86.59	
CENDL-3	79.83	
Mughabghab et al. [Mu81]	80±2	recommendation
Hay [Ha58]	67±7	
Vertebnyj et al. [Ve74]	80±2	
(n,α)		
Present	0.0200	
JENDL-3.3	0.0174	
ENDF/B-VI	1.91×10^{-5}	
JEFF-3.0	0.0	
CENDL-3	0.0174	
Mughabghab et al. [Mu81]	0.0174±0.0016	recommendation
Cheifetz et al. [Ch62]	0.016±0.003	Maxw. average
Asghar et al. [As78]	0.0223±0.0020	Maxw. average
Total		
Present	413.65	
JENDL-3.3	405.03	
ENDF/B-VI	405.25	
JEFF-3.0	422.48	
CENDL-3	402.91	
Hay [Ha58]	410±20	
Vertebnyj et al. [Ve74]	418±7	

Table 3.2 Resonance integrals of ^{143}Nd capture cross section

Unit: barns

Present	143	
JENDL-3.3	129	
ENDF/B-VI	131	
JEFF-3.0	133	
CENDL-3	130	
Mughabghab et al. [Mu03]	130±30	recommendation

Table 3.3 Optical potential parameters for n+^{143}Nd reaction

For the previous evaluation

Potential shape: Derivative Woods-Saxon for surface-imaginary part

Depth (MeV)	Radius (fm)	Diffuseness (fm)
V = 45.76	6.746	0.6
W_S = 6.97	6.432	0.45
V_{SO} = 7.0	6.694	0.6

For the present evaluation

Potential shape: Derivative Woods-Saxon for surface-imaginary part

Depth (MeV)	Radius (fm)	Diffuseness (fm)
$V = 46.59 - 0.417\times E$	$1.172\times A^{1/3}+0.6$	0.62
$W_I = 0.125\times E - 0.0004\times E^2$	$1.16\times A^{1/3}+0.6$	0.62
W_S = 7.486	$1.16\times A^{1/3}+1.1$	0.35
V_{SO} = 7.0	$1.16\times A^{1/3}+0.6$	0.62

A: mass number

Table 3.4 Parameters used in CASTHY calculation for ^{143}Nd

a) Level density parameters

Nuclide	a(1/MeV)	T(MeV)	spin-cutoff	Ex(MeV)	Pairing(MeV)
143Nd	19.2	0.450	17.49	3.52	1.18
144Nd	17.2	0.580	16.64	5.79	1.94

b) Gamma-ray strength function

1.65×10^{-3} adjusted to reproduce the capture cross section of about 147 mb at 65 keV

c) Excited levels

No.	Energy(MeV)	Spin-parity		
0	0.0	7/2	−	
1	0.74205	3/2	−	*
2	1.22804	13/2	+	
3	1.30586	1/2	−	
4	1.40708	9/2	−	*
5	1.43123	11/2	−	*
6	1.506	9/2	+	taken from RIPL-2
7	1.55554	5/2	−	*
8	1.55644	3/2	+	
9	1.60838	1/2	+	
10	1.73921	9/2	−	
11	1.77485	1/2	+	
12	1.79952	3/2	+	
13	1.8515	7/2	−	*
14	1.85256	3/2	−	
15	1.91081	5/2	−	
16	1.9666	5/2	+	
17	1.98822	11/2	−	
18	1.99640	5/2	+	
19	2.00467	1/2	−	
20	2.0113	9/2	+	
21	2.01837	15/2	−	
22	2.0192	5/2	−	
23	2.03560	7/2	−	
24	2.06385	7/2	+	
25	2.06684	13/2	−	
26	2.07513	11/2	−	
27	2.09060	7/2	+	
28	2.09439	11/2	−	
29	2.101	7/2	−	
30	2.12582			continuum

Direct inelastic scattering was calculated to the levels with "*".

Table 3.5 Maxwellian-averaged ^{143}Nd capture cross section

Unit: mb

	10 keV	30 keV
Present	512	245
JENDL-3.3	564	288
ENDF/B-VI	502	239
JEFF-3	528	275
CENDL-3	576	281
Wisshak et al. [Wi97b]	537	244

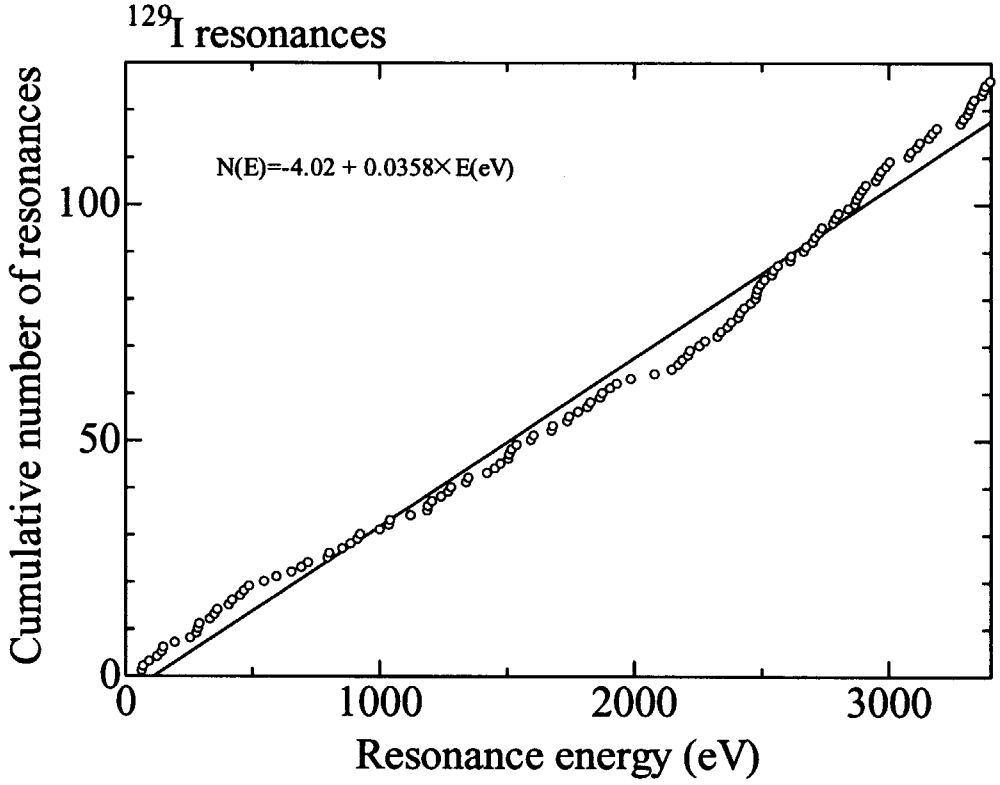

Fig. 2.1 Cumulative numbers of resolved resonances of ^{129}I

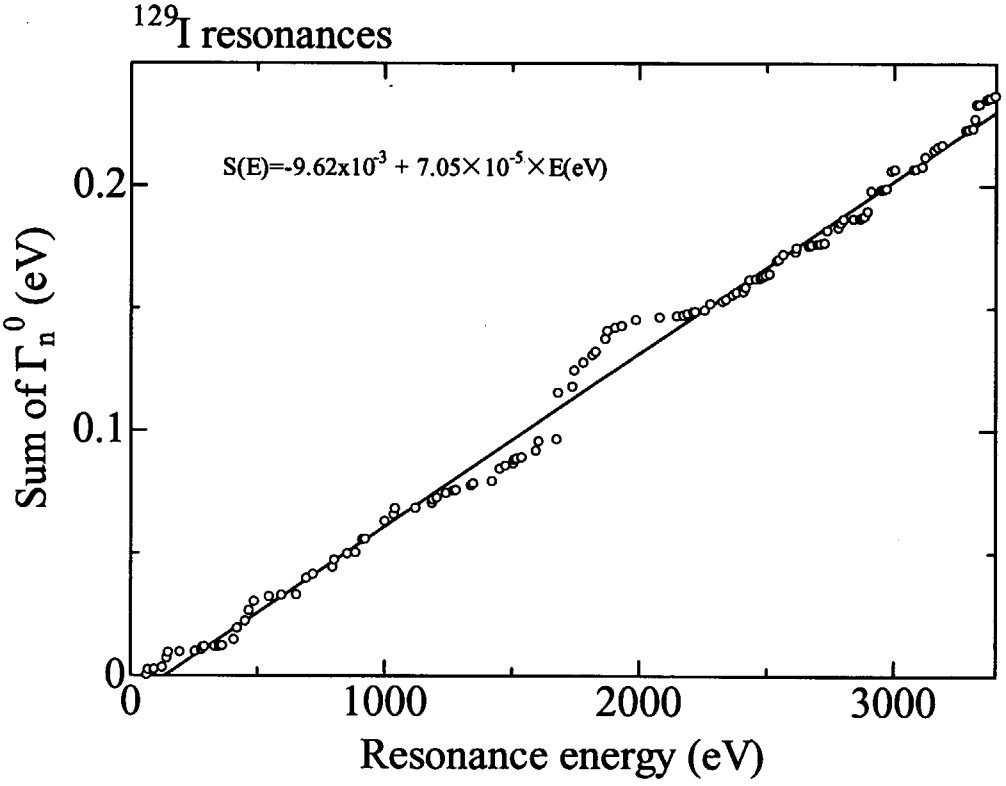

Fig. 2.2 Cumulative sum of reduced neutron widths

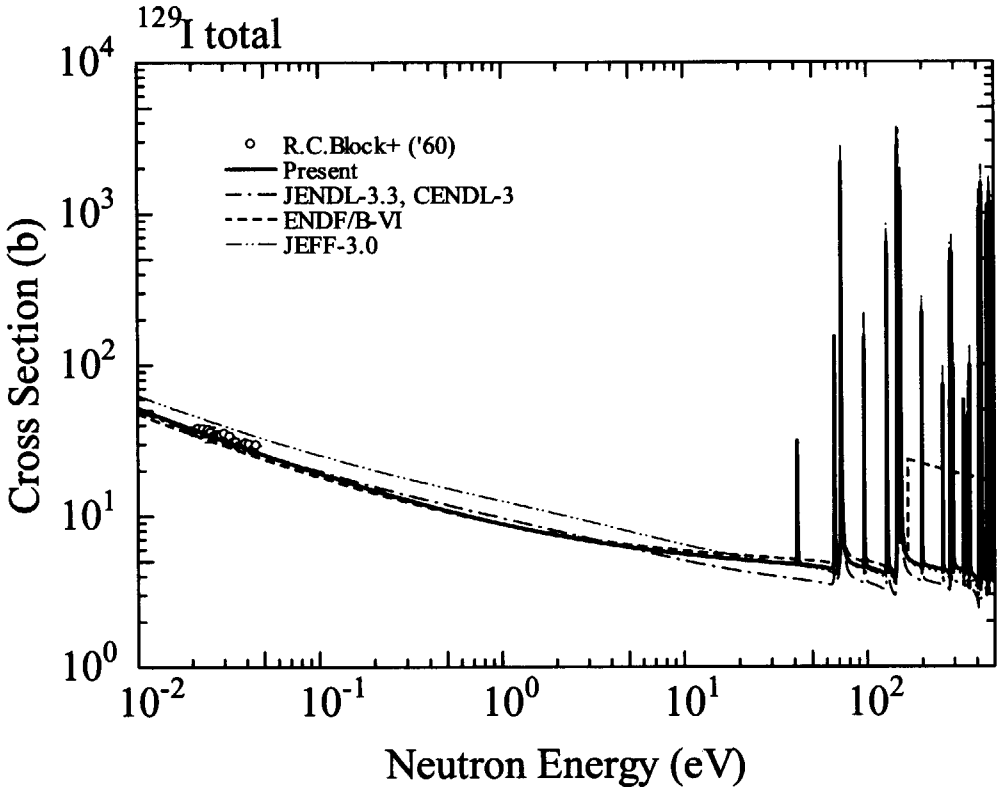

Fig. 2.3 ^{129}I total cross section (below 500 eV)

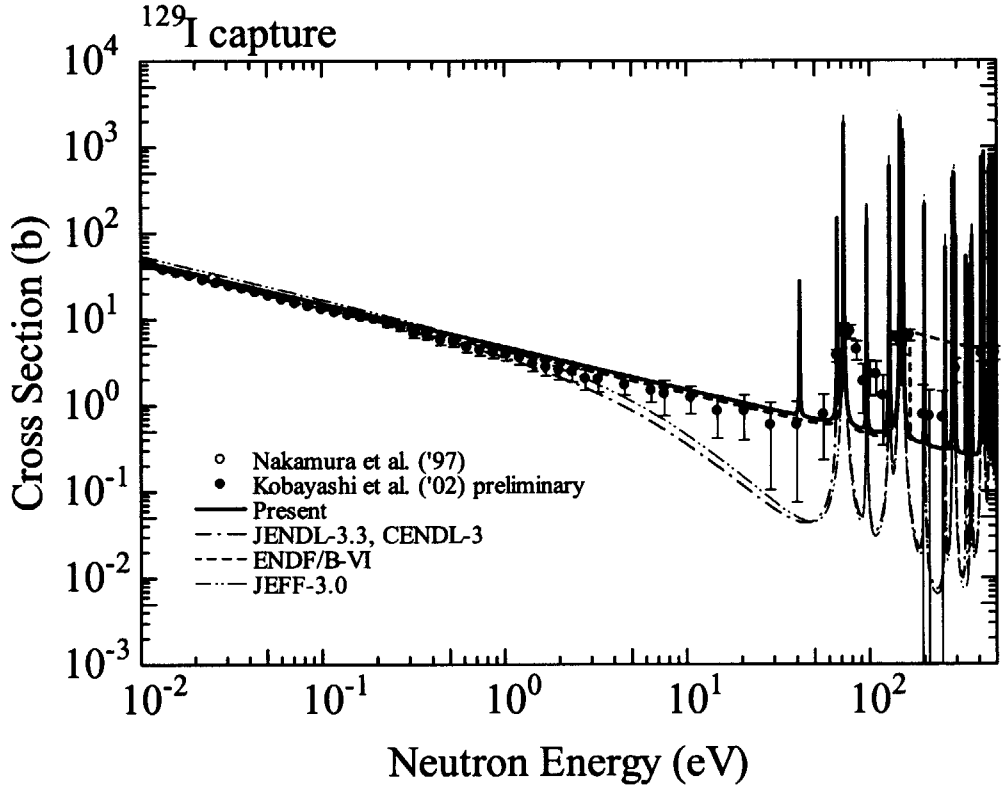

Fig. 2.4 ^{129}I capture cross section (below 500 eV)

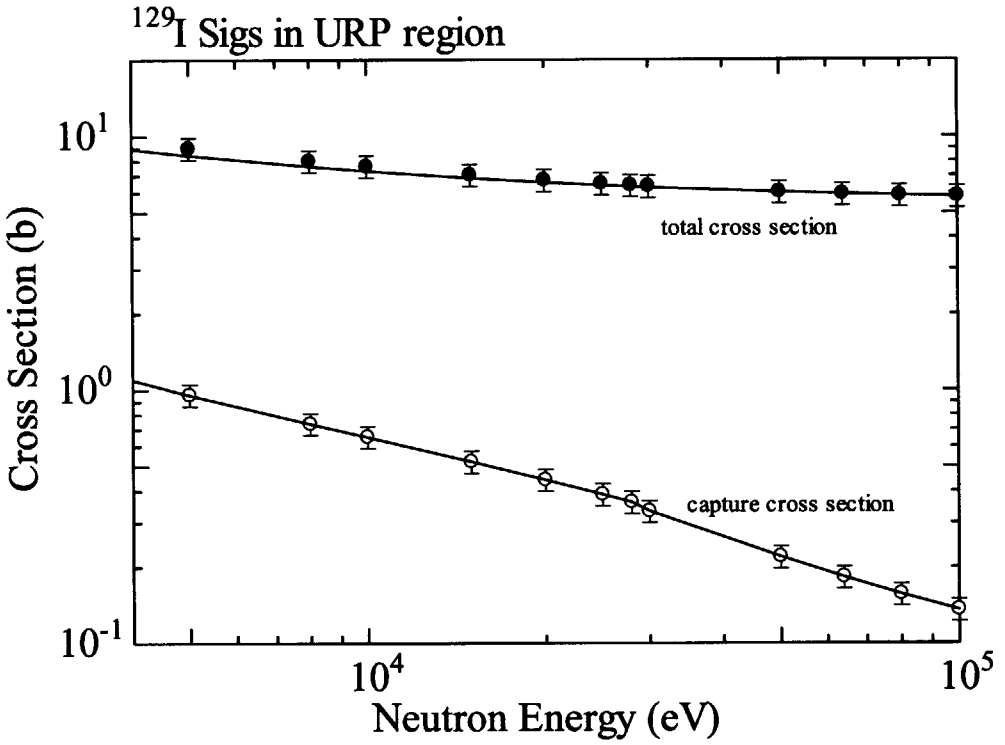

Fig. 2.5 Cross sections of ^{129}I in the unresolved resonance region

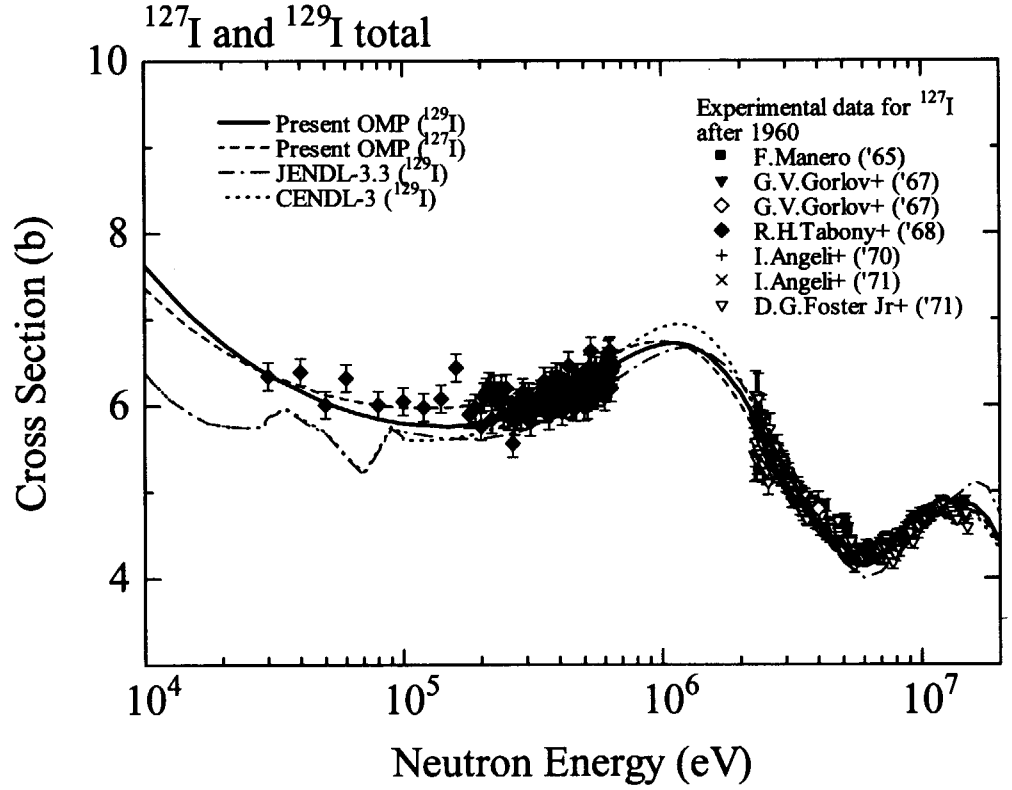

Fig. 2.6 Total cross sections of ^{127}I and ^{129}I

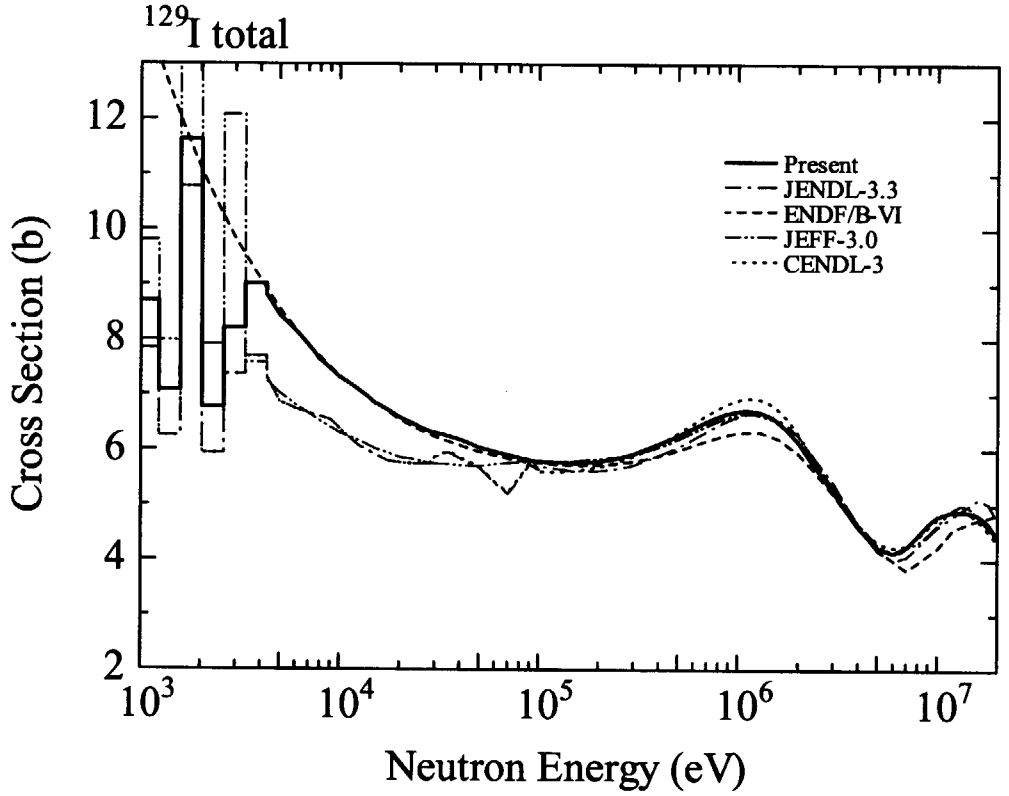

Fig. 2.7 Total cross sections of ^{129}I

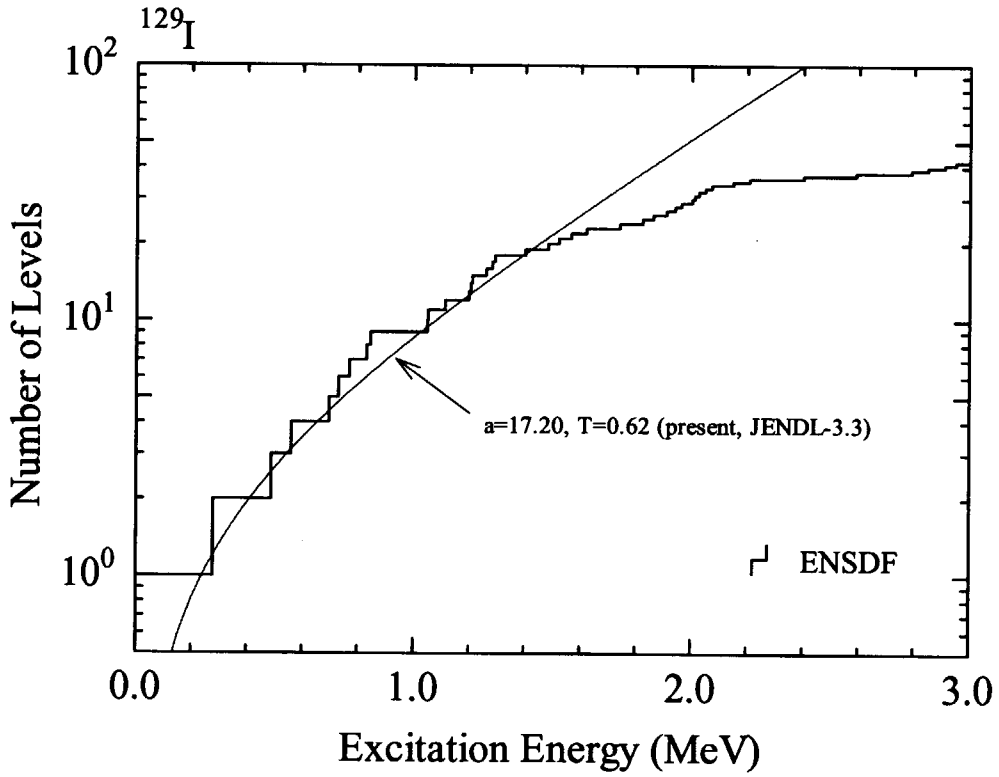

Fig. 2.8 Example of level density parameters (^{129}I)

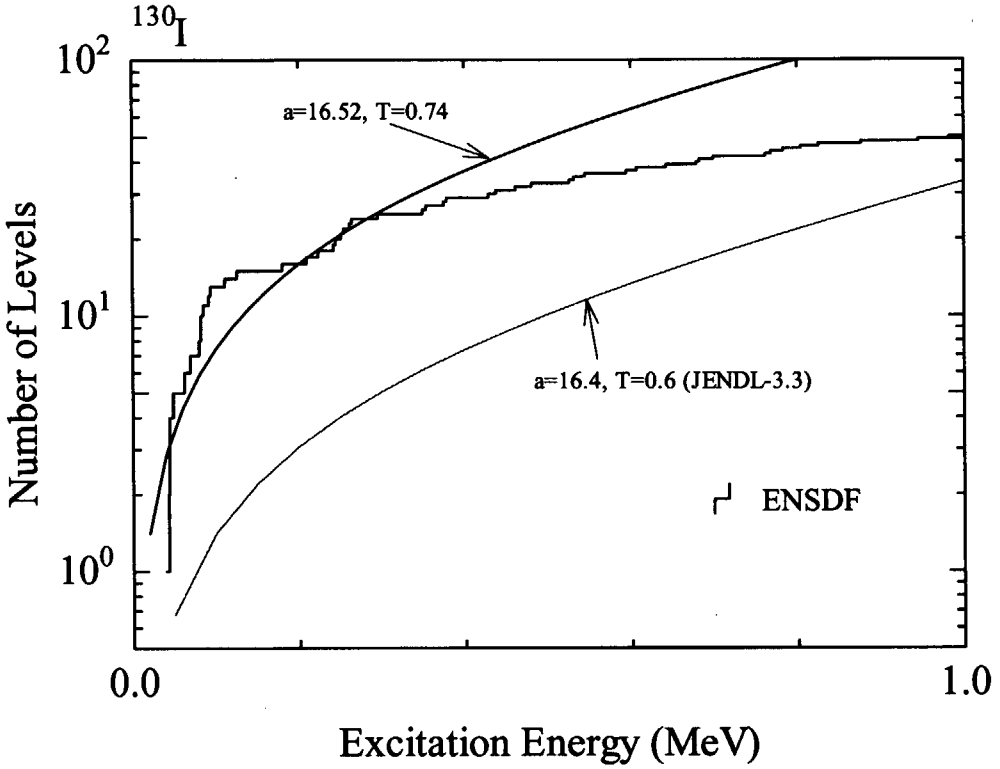

Fig. 2.9 Example of level density parameters (^{130}I)

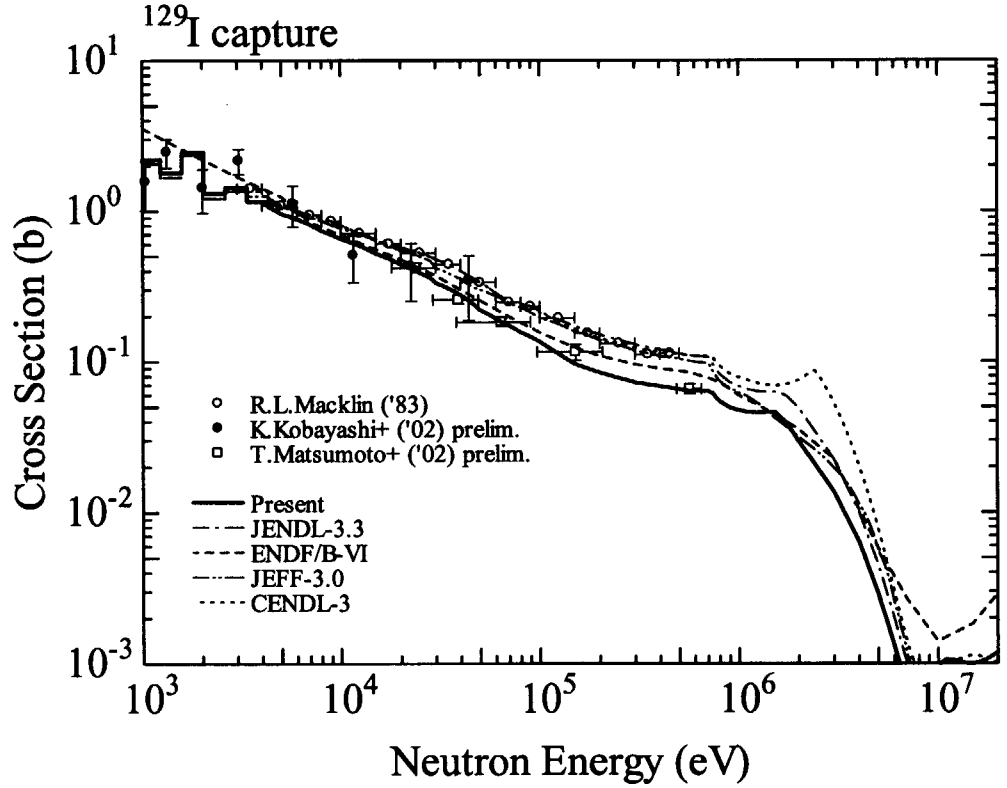

Fig. 2.10 ^{129}I capture cross section

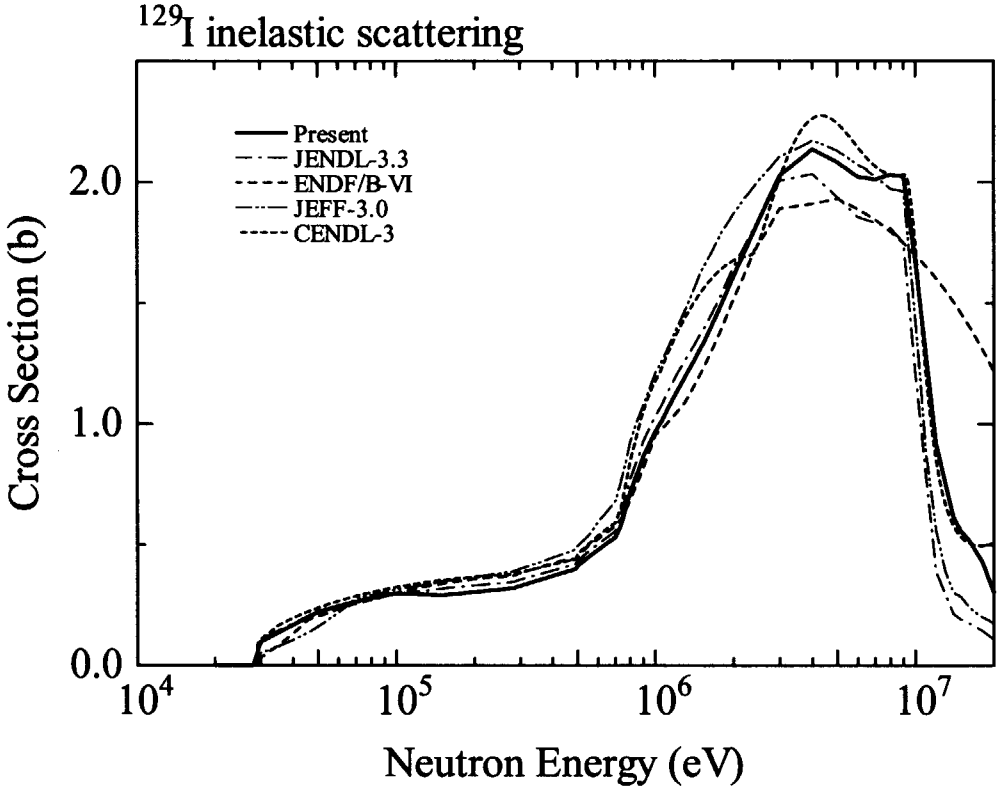

Fig. 2.11 Total inelastic scattering cross section of ^{129}I

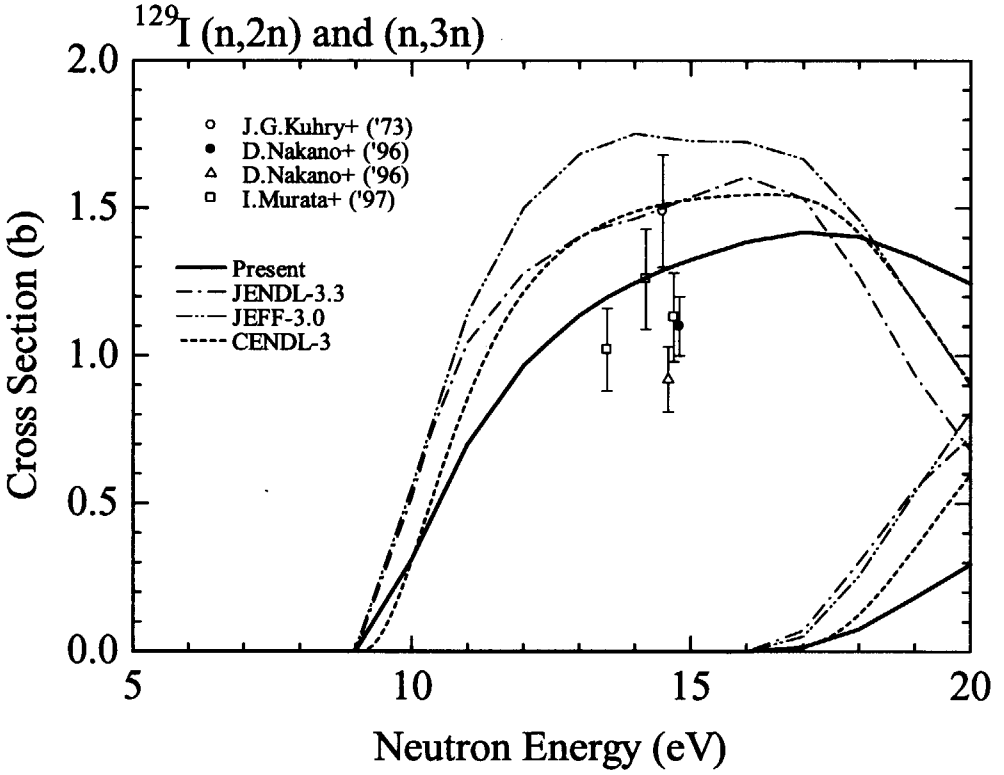

Fig. 2.12 ^{129}I(n,2n) and (n,3n) reaction cross sections

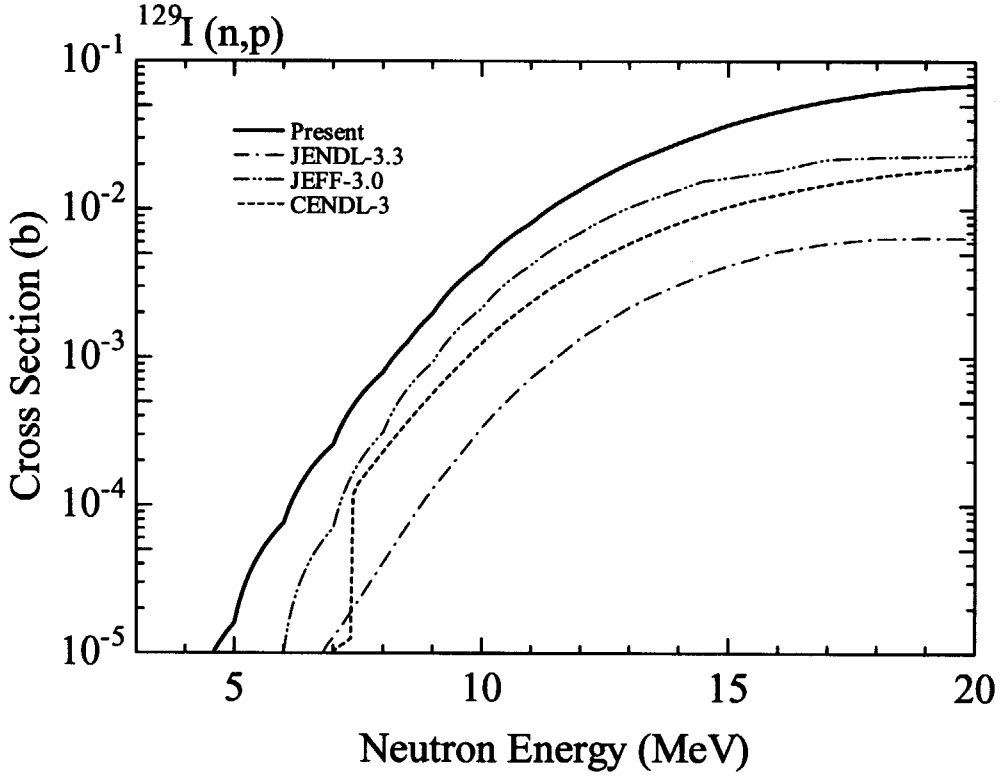

Fig. 2.13 ^{129}I(n,p) reaction cross section

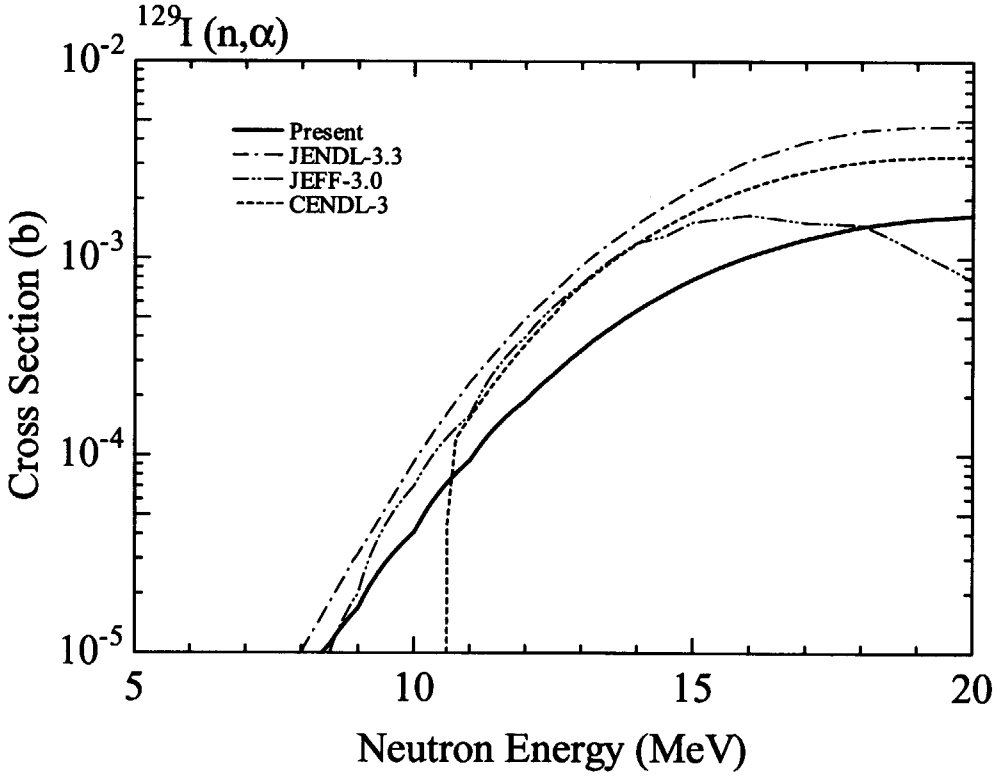

Fig. 2.14 ^{129}I(n,α) reaction cross section

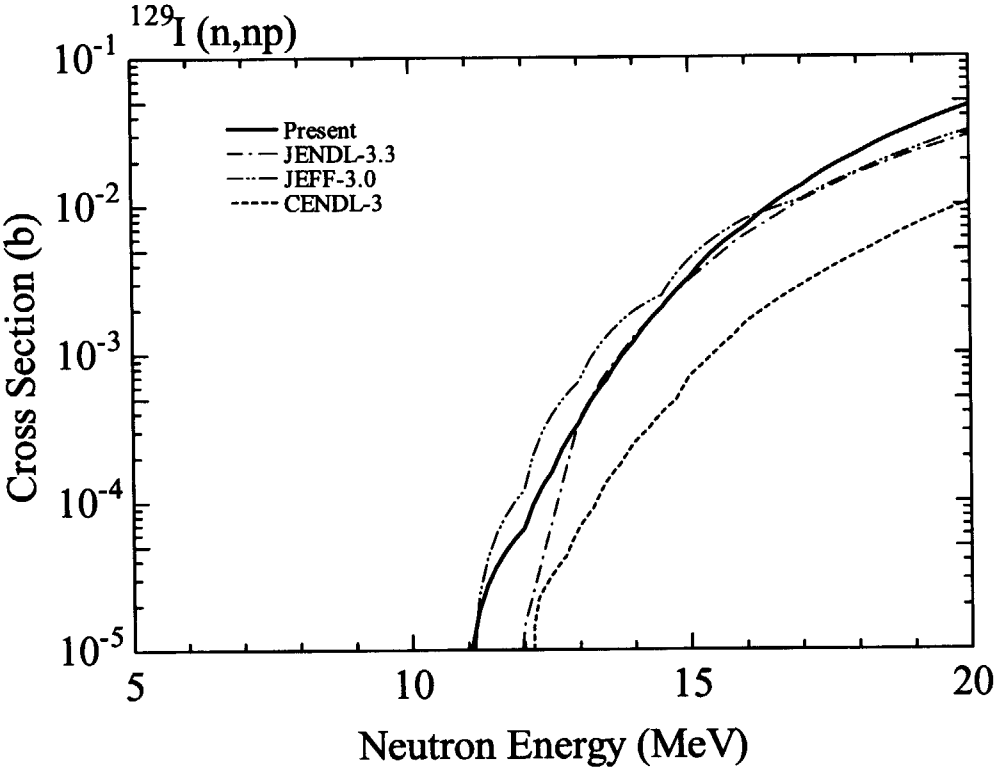

Fig. 2.15 ^{129}I(n,np) reaction cross section

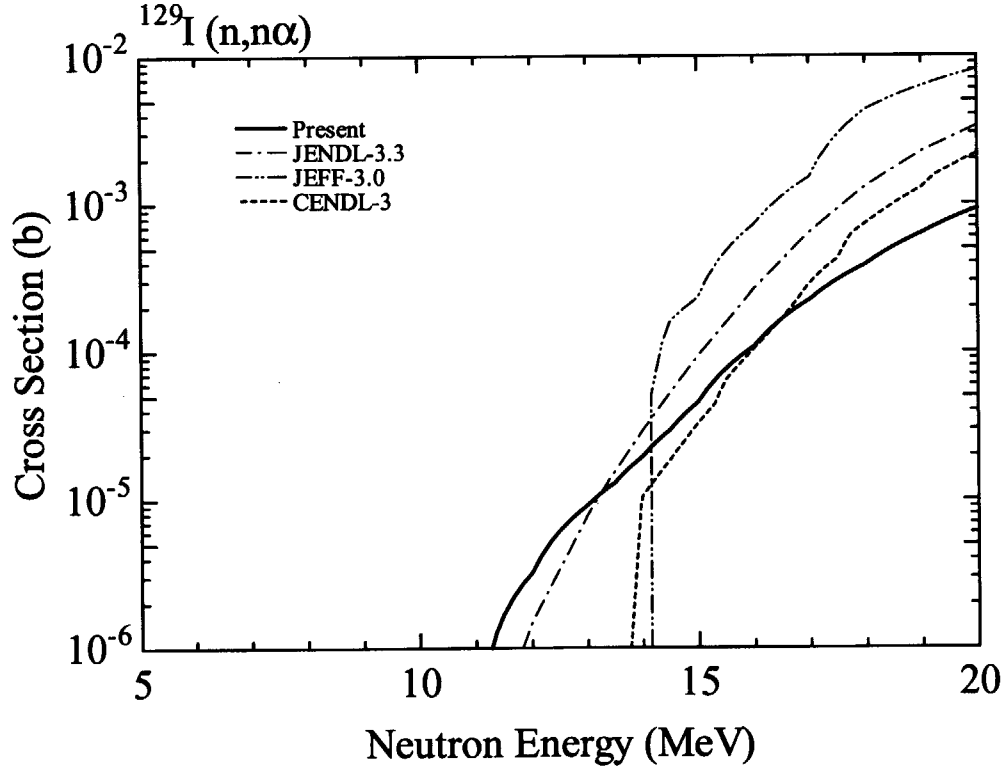

Fig. 2.16 ^{129}I(n,nα) reaction cross section

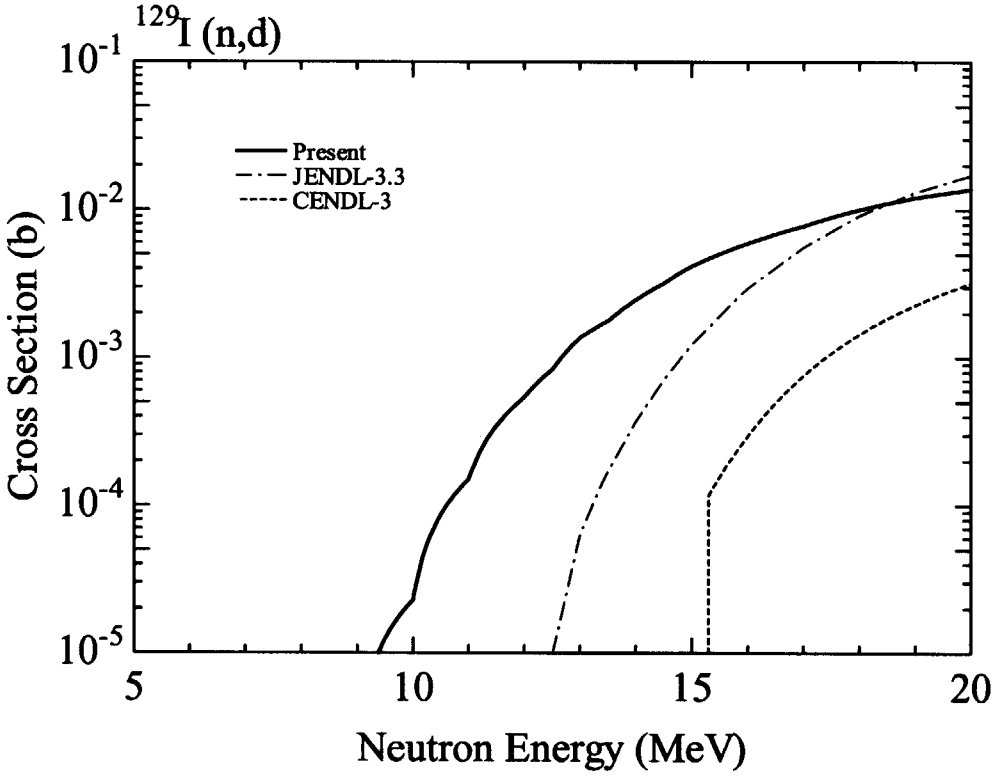

Fig. 2.17 ^{129}I(n,d) reaction cross section

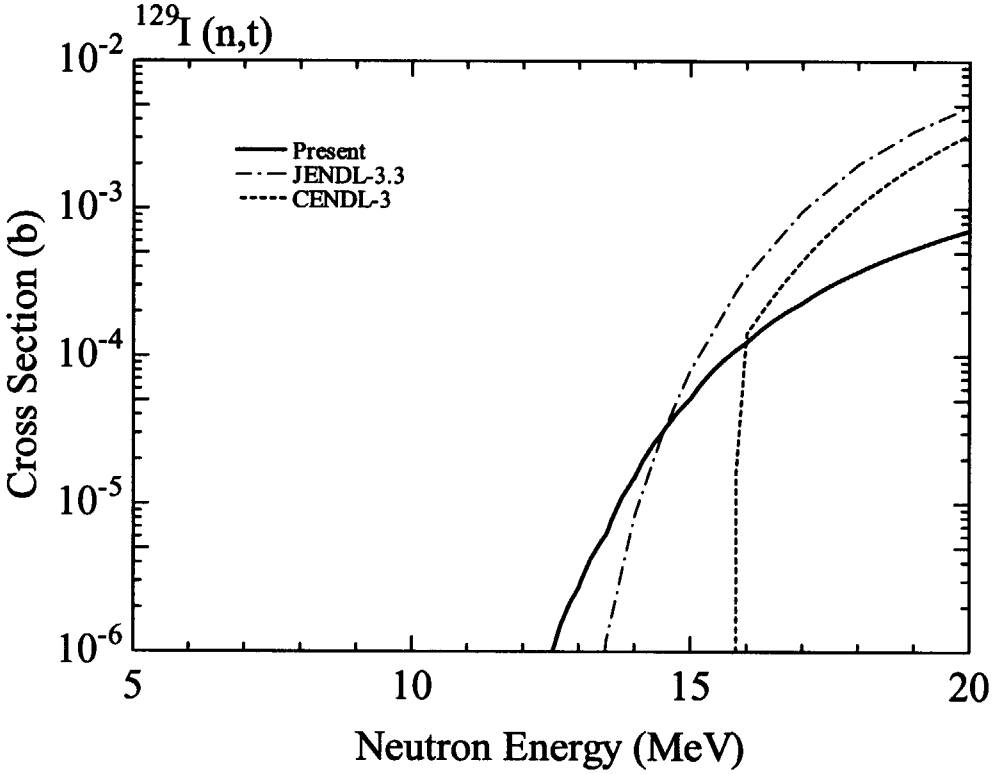

Fig. 2.18 ^{129}I(n,t) reaction cross section

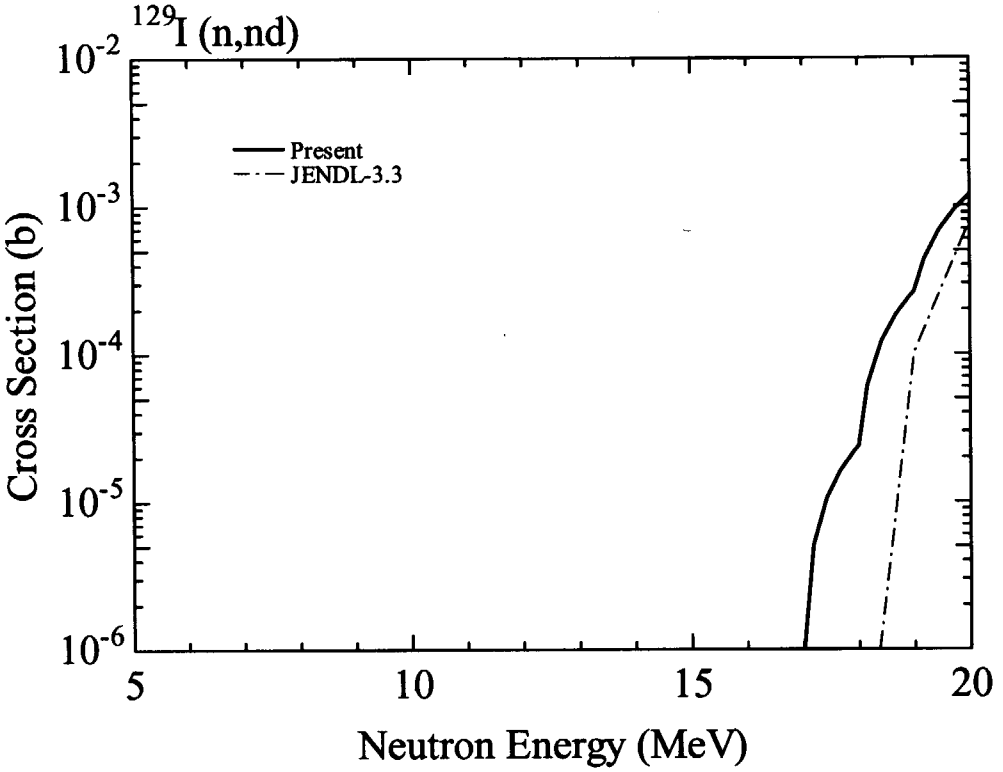

Fig. 2.19 ^{129}I(n,nd) reaction cross section

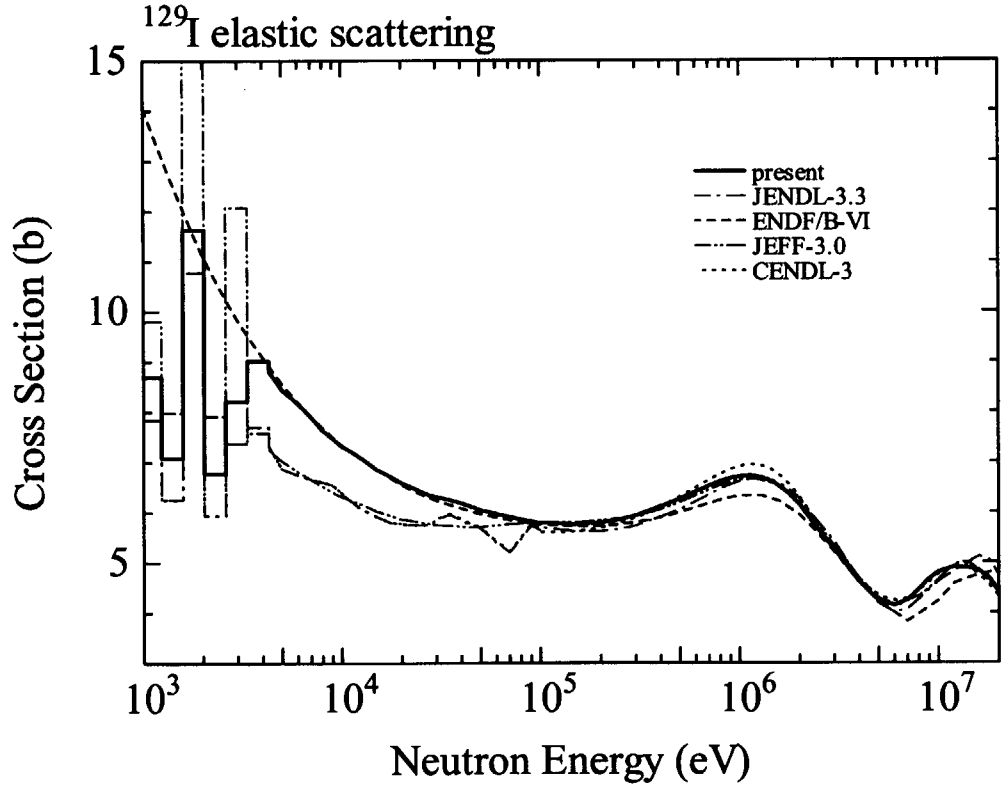

Fig. 2.20 ^{129}I elastic scattering cross section

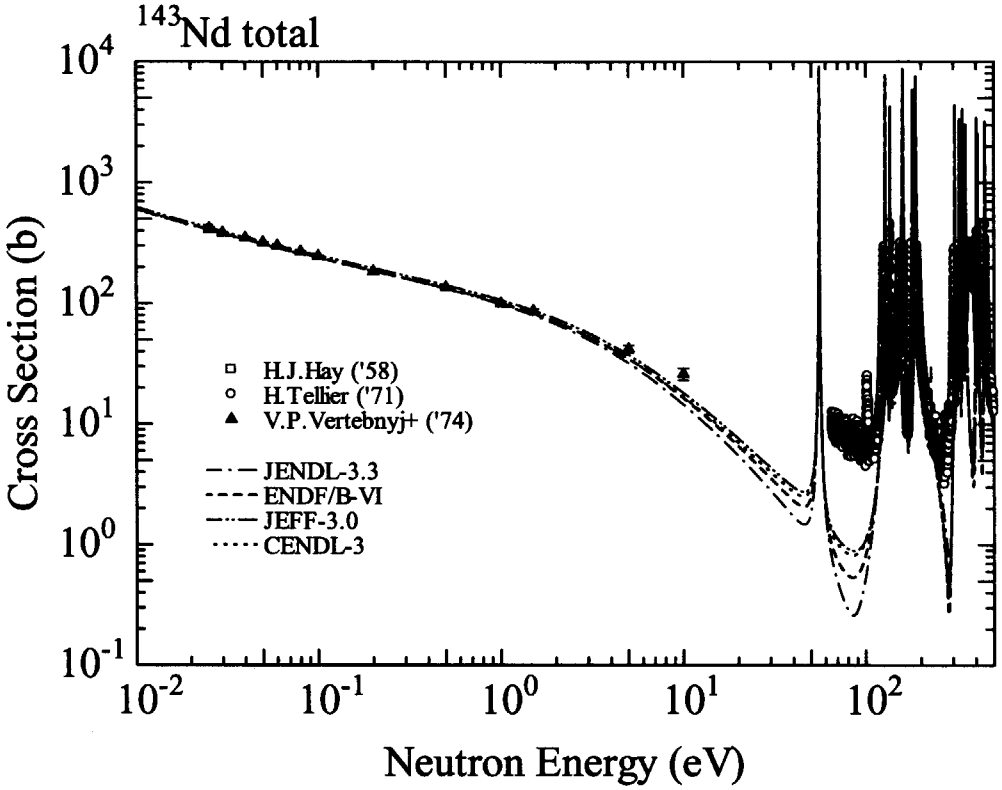

Fig. 3.1 Total cross section of ^{143}Nd (below 500 eV)

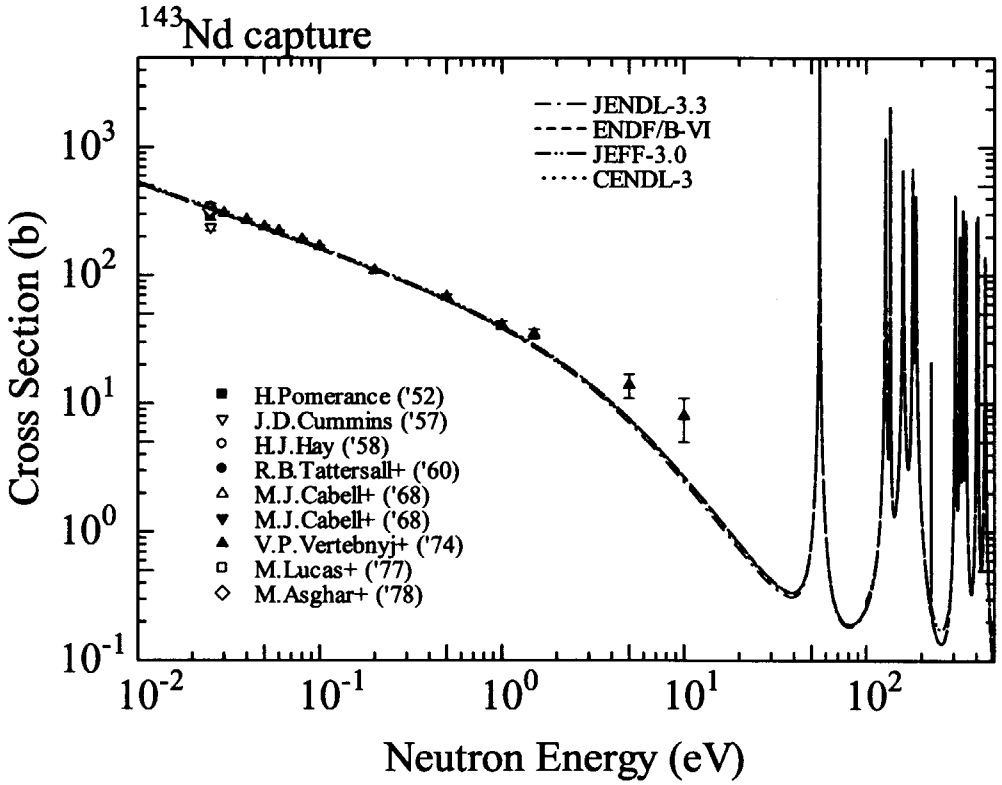

Fig. 3.2 Capture cross section of ^{143}Nd (below 500 eV)

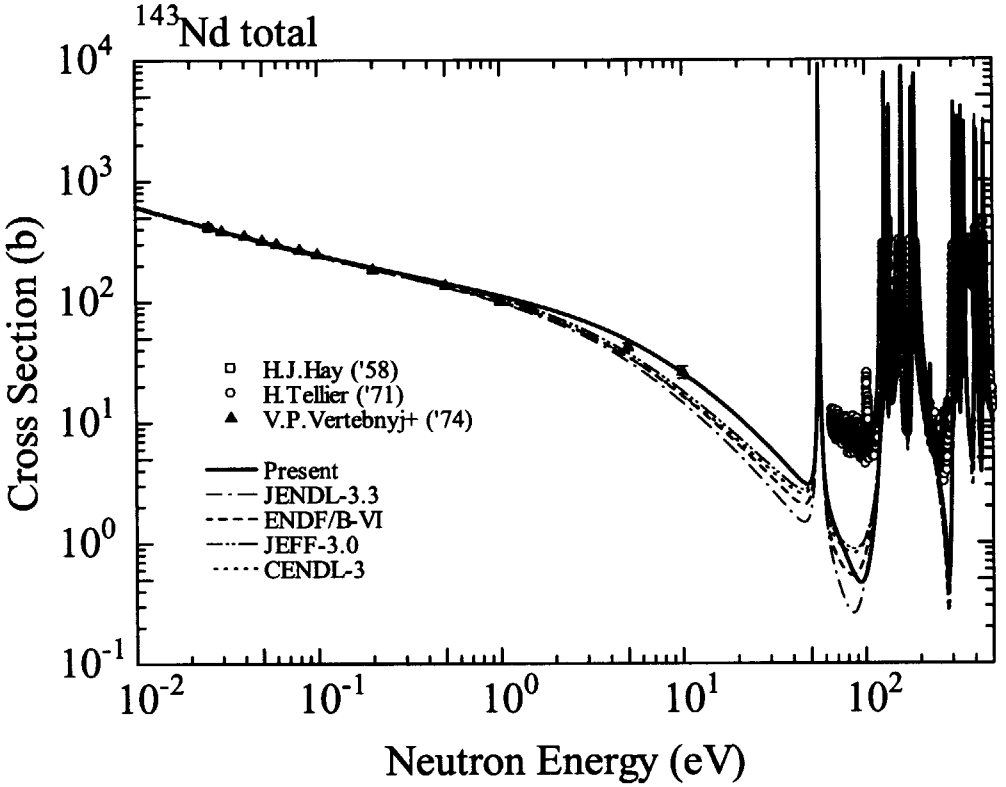

Fig. 3.3 Total cross section of ^{143}Nd (below 500 eV)

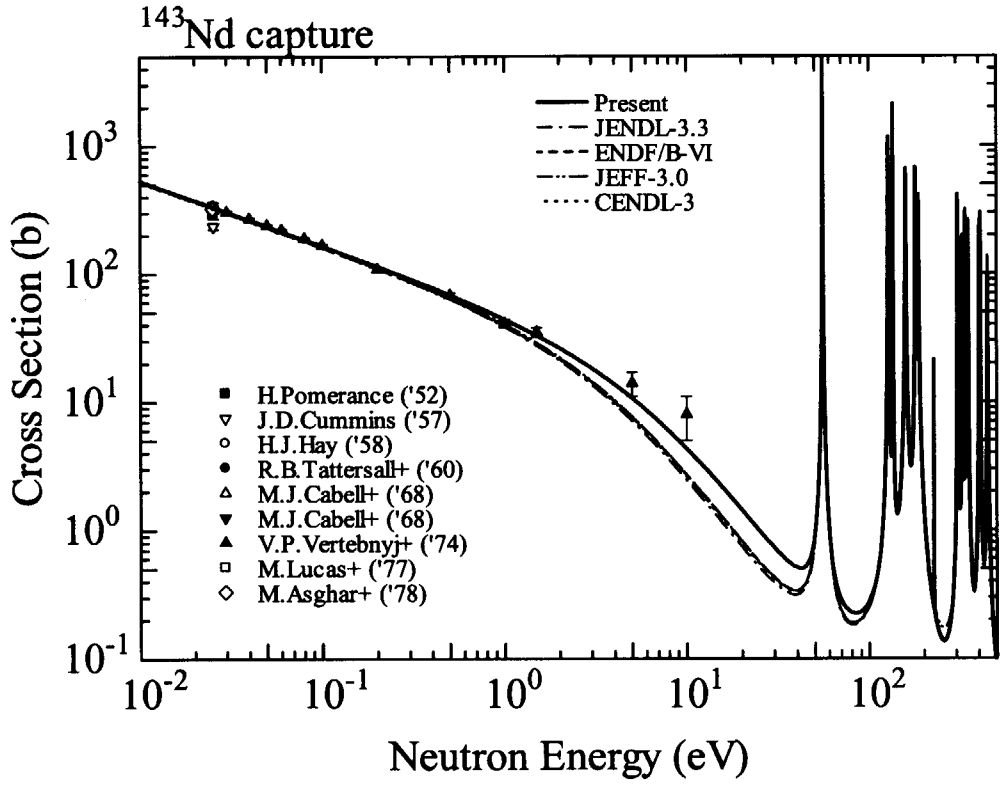

Fig. 3.4 Capture cross section of ^{143}Nd (below 500 eV)

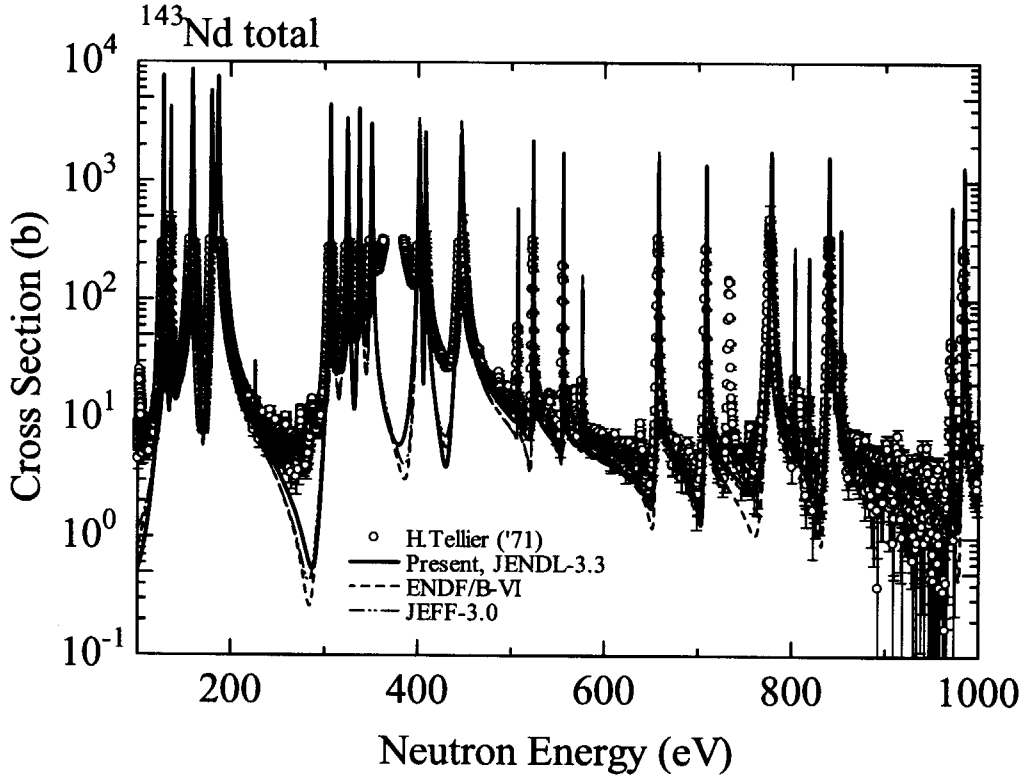

Fig. 3.5(a) Total cross section of ^{143}Nd (100 eV to 1 keV)

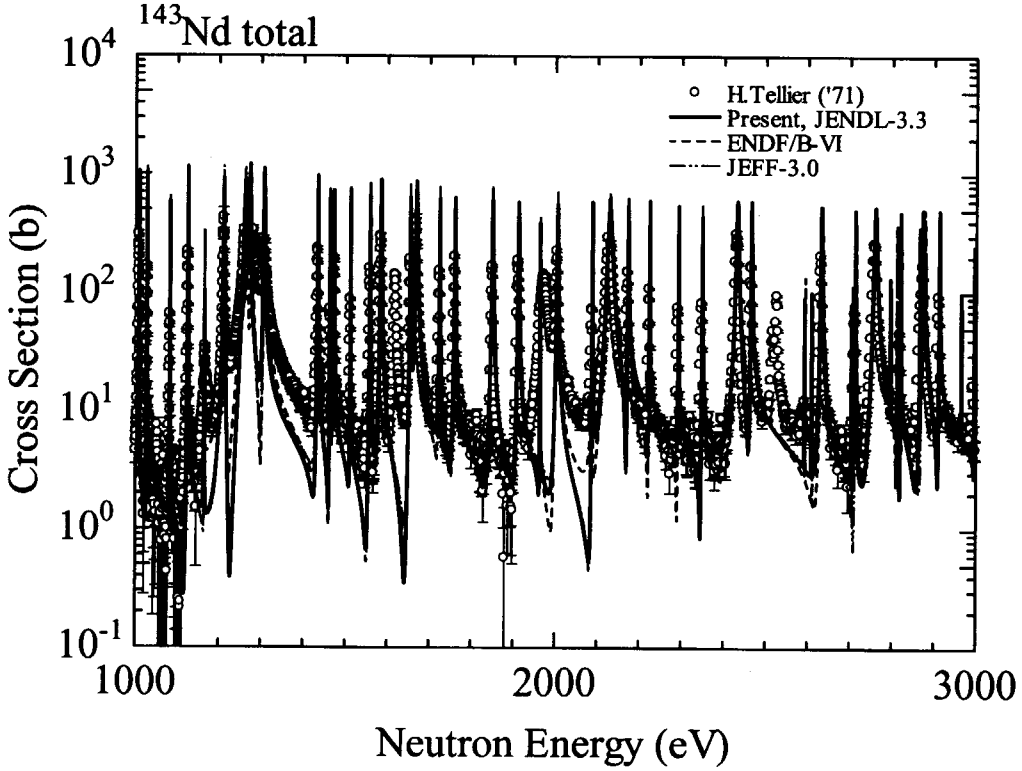

Fig. 3.5(b) Total cross section of ^{143}Nd (1 to 3 keV)

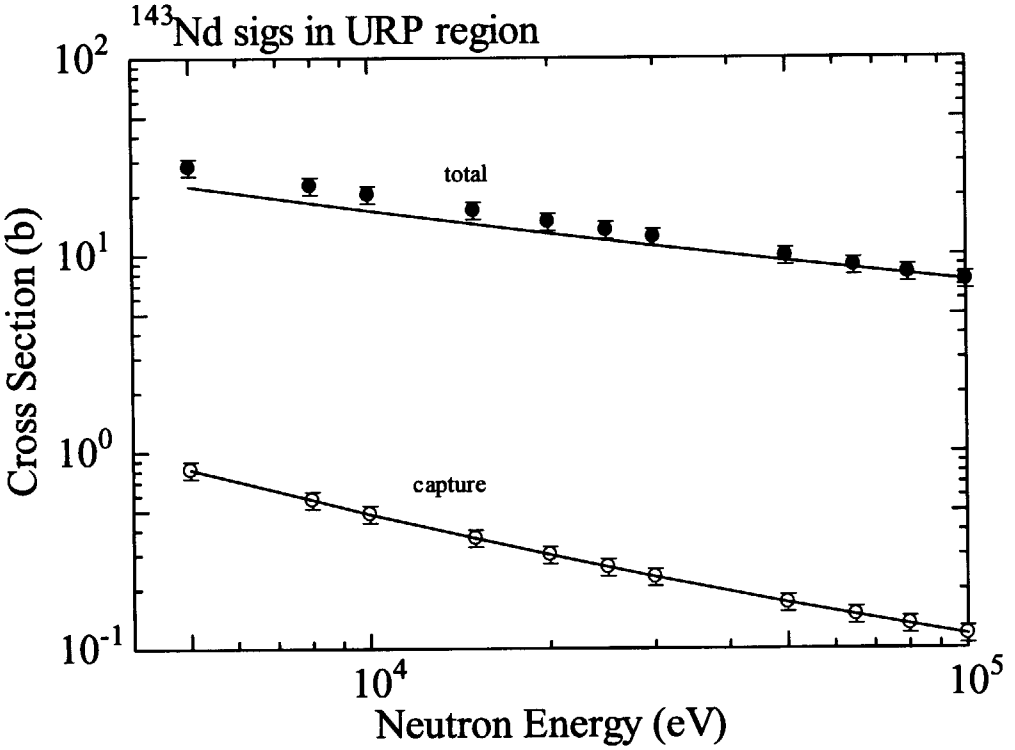

Fig. 3.6 Cross sections of ^{143}Nd in the unresolved resonance region

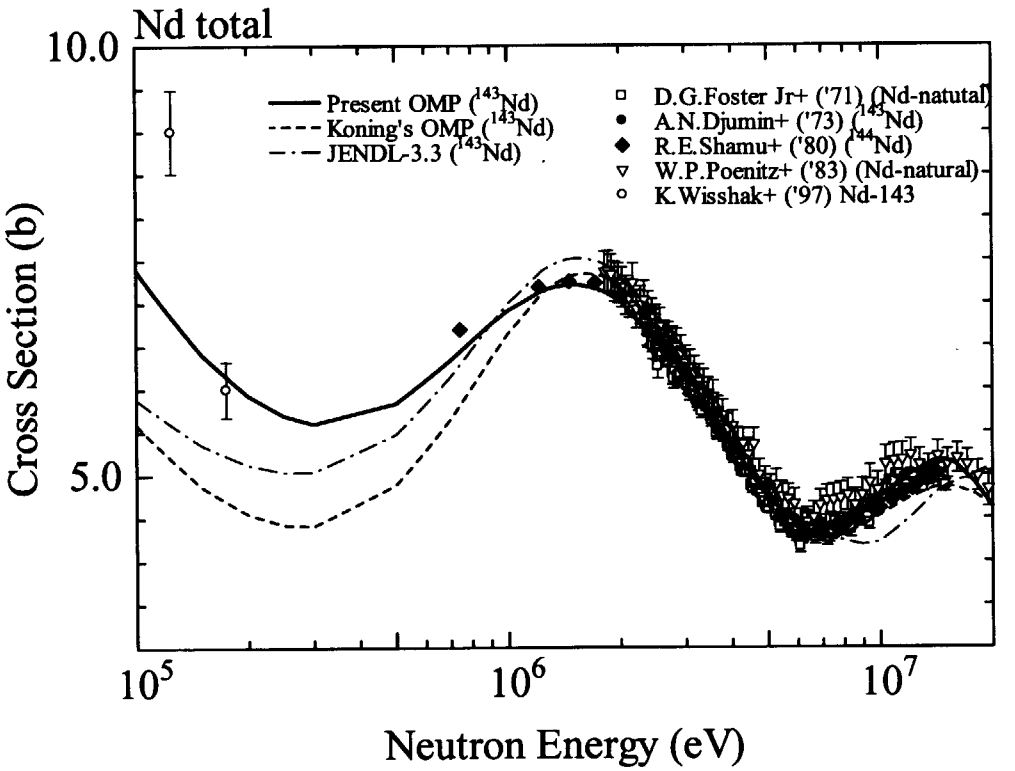

Fig. 3.7 Total cross section of Nd

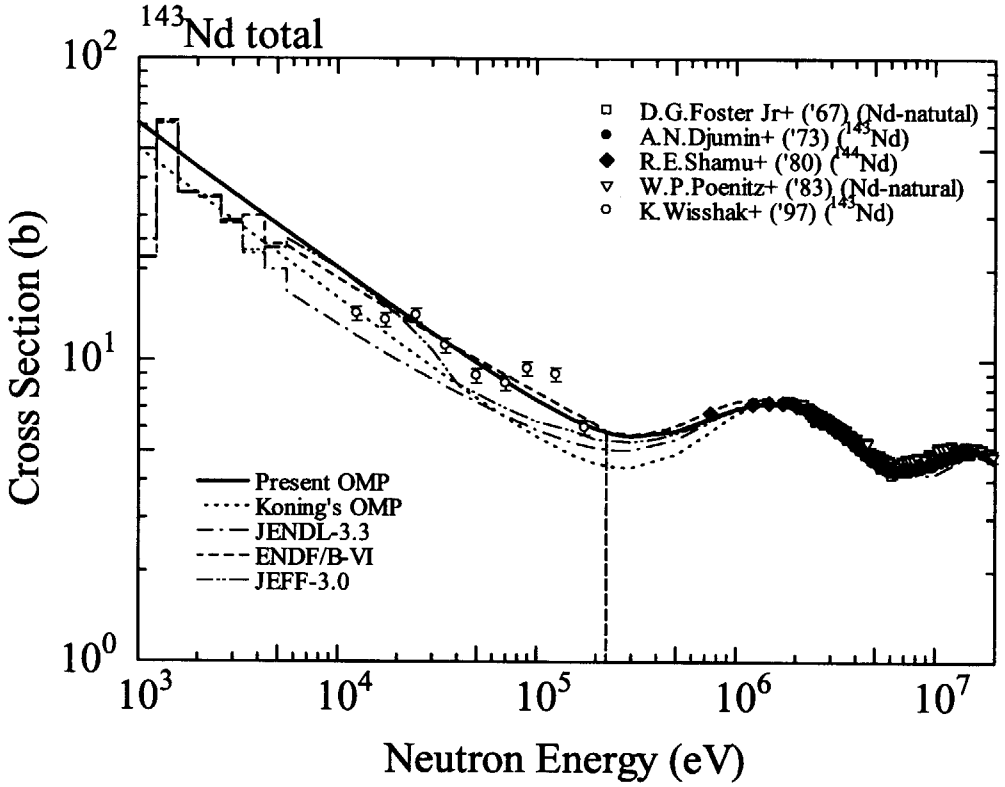

Fig. 3.8 Total cross section of ^{143}Nd

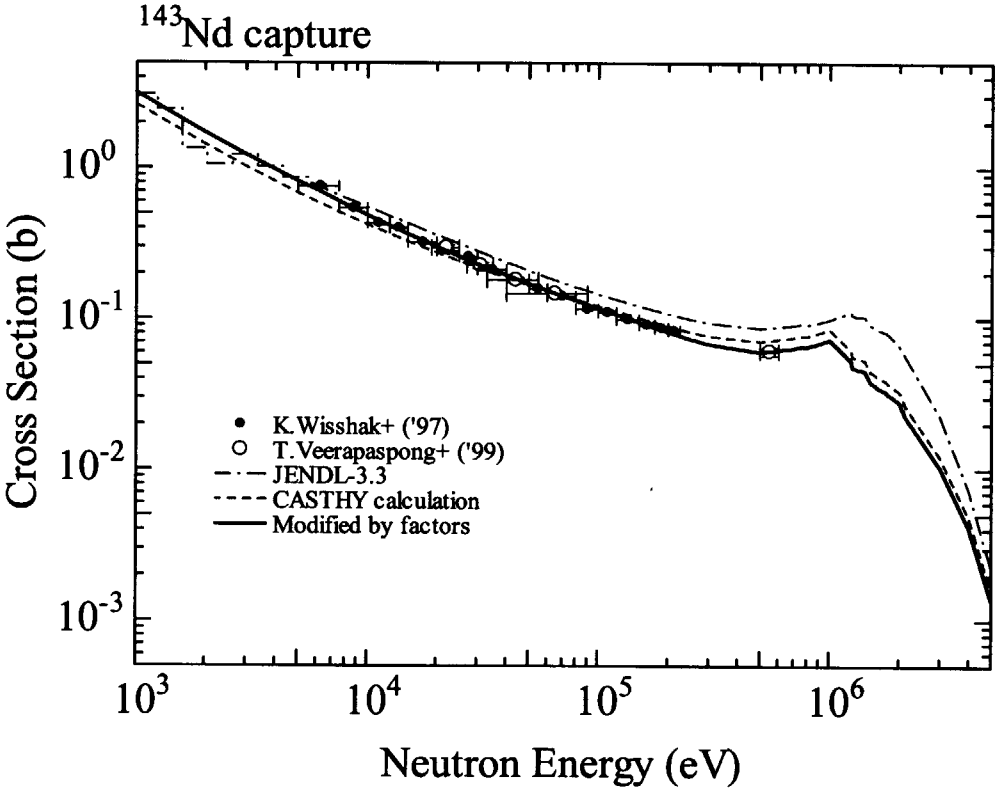

Fig. 3.9 Capture cross section of ^{143}Nd (CASTHY calculation)

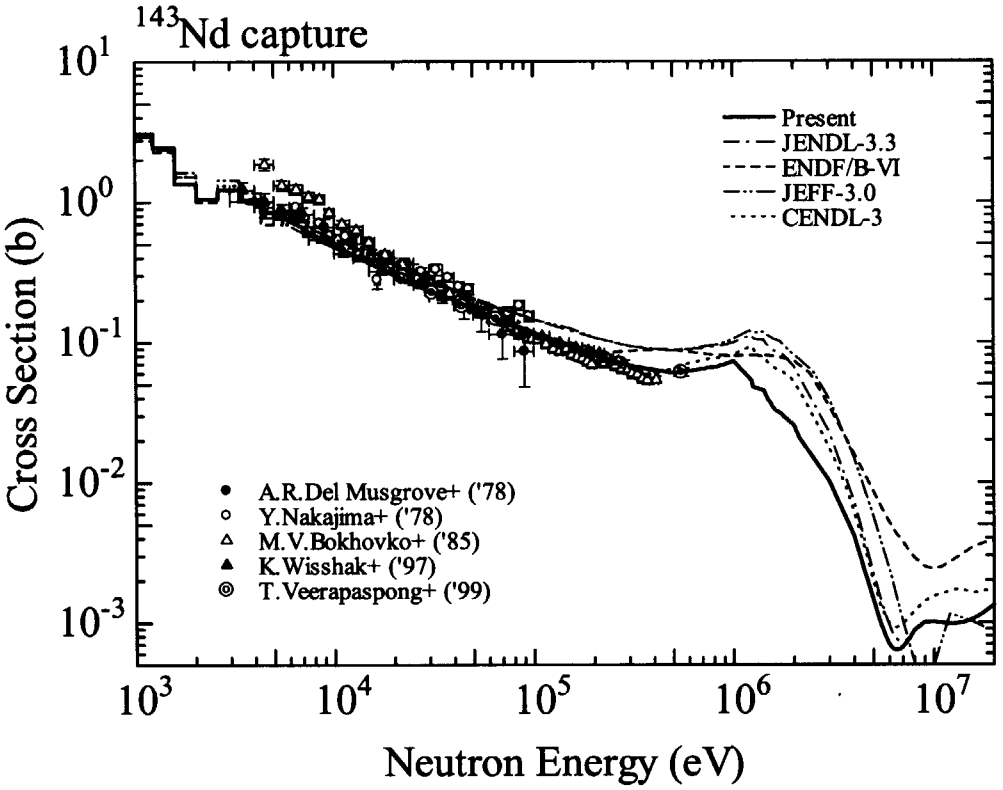

Fig. 3.10 ^{143}Nd capture cross section

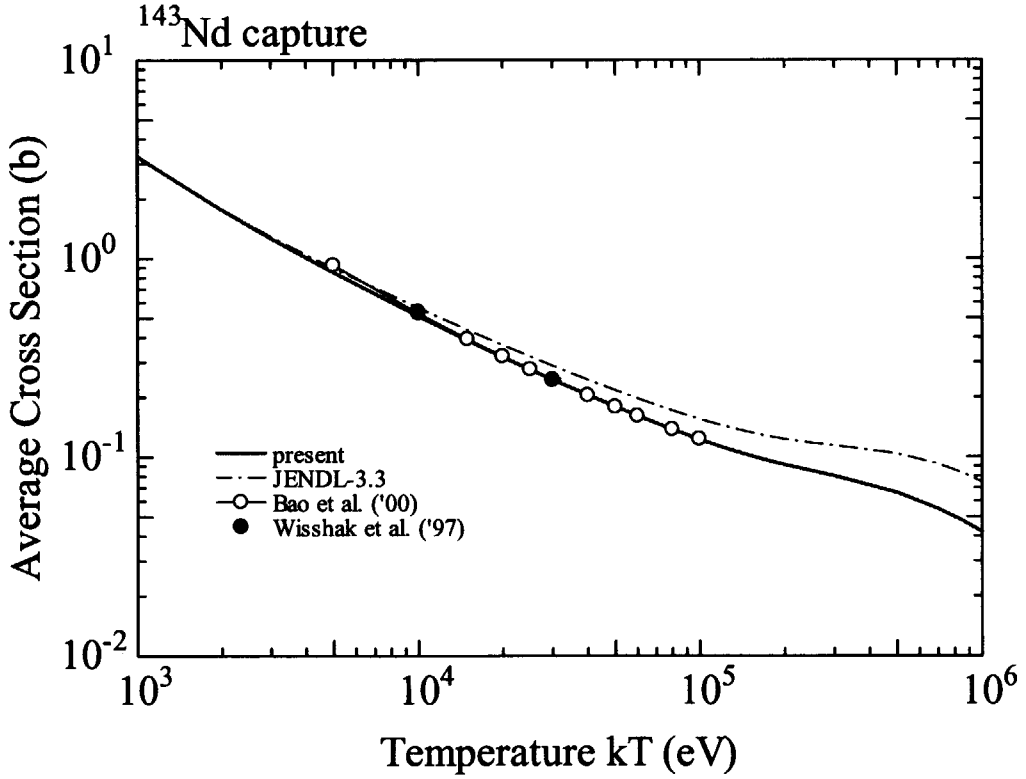

Fig. 3.11 Maxwellian spectrum averaged ^{143}Nd capture cross section

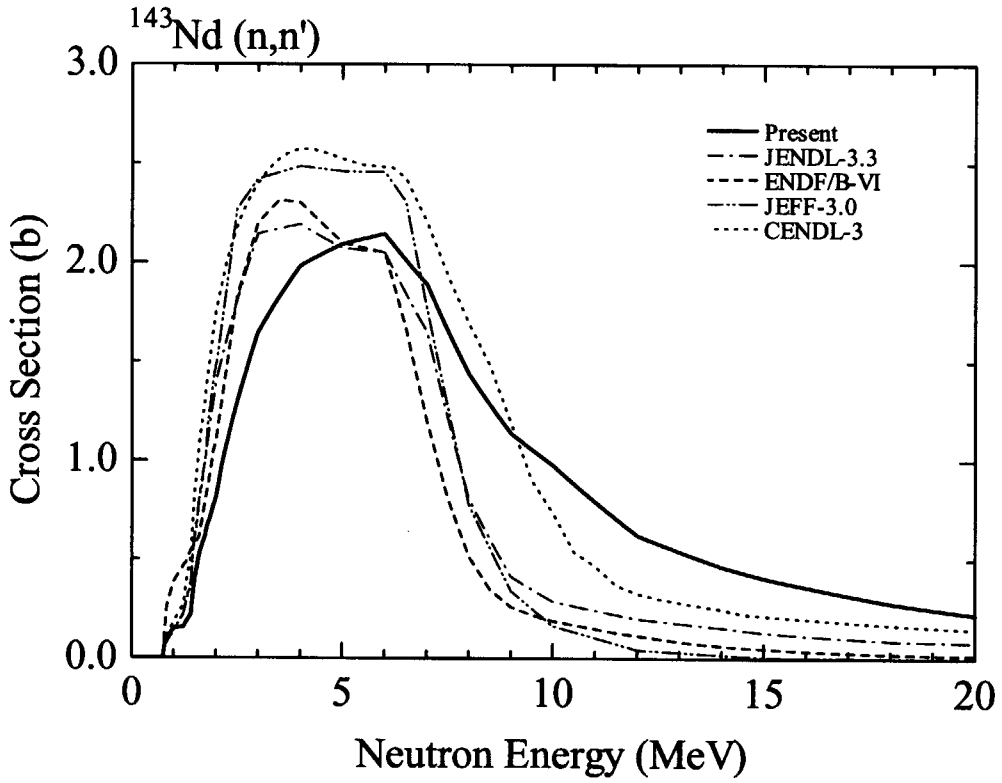

Fig. 3.12 ^{143}Nd total inelastic scattering cross section

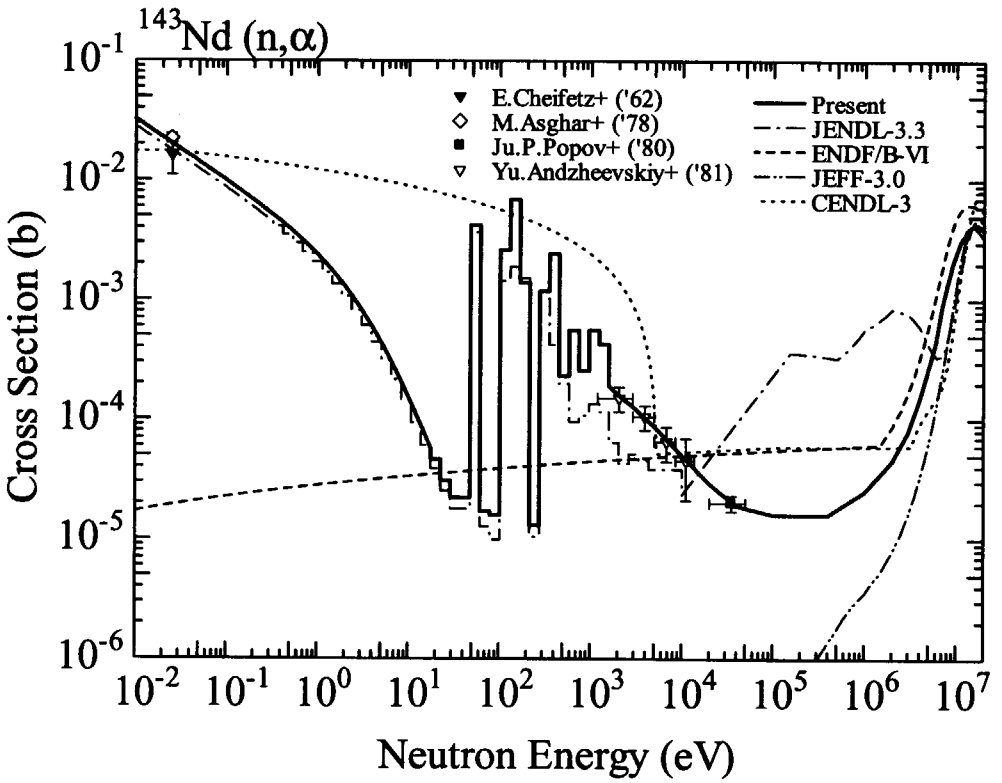

Fig. 3.13 ^{143}Nd(n,α) reaction cross section

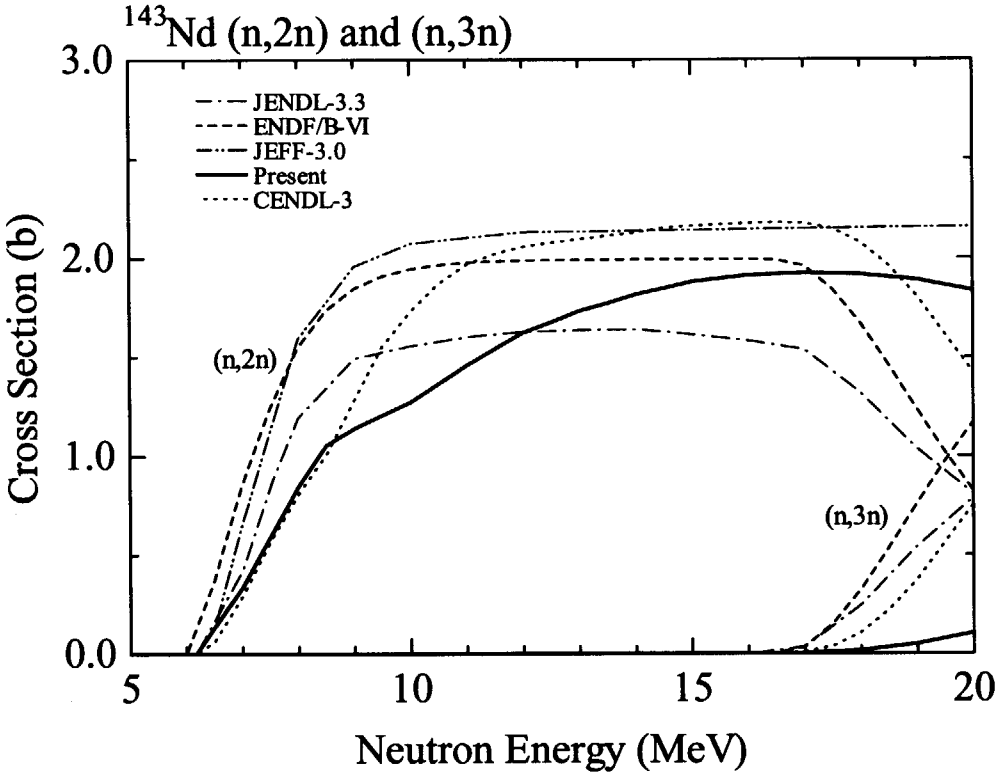

Fig. 3.14 ^{143}Nd(n,2n) and (n,3n) reaction cross section

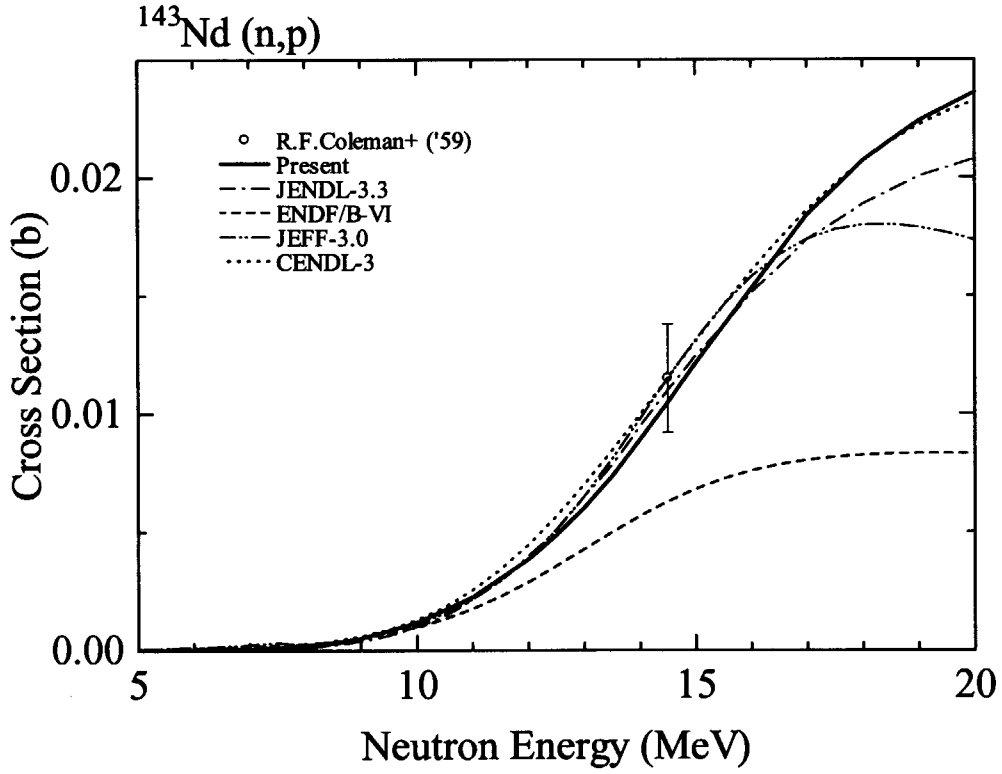

Fig. 3.15 ^{143}Nd(n,p) reaction cross section

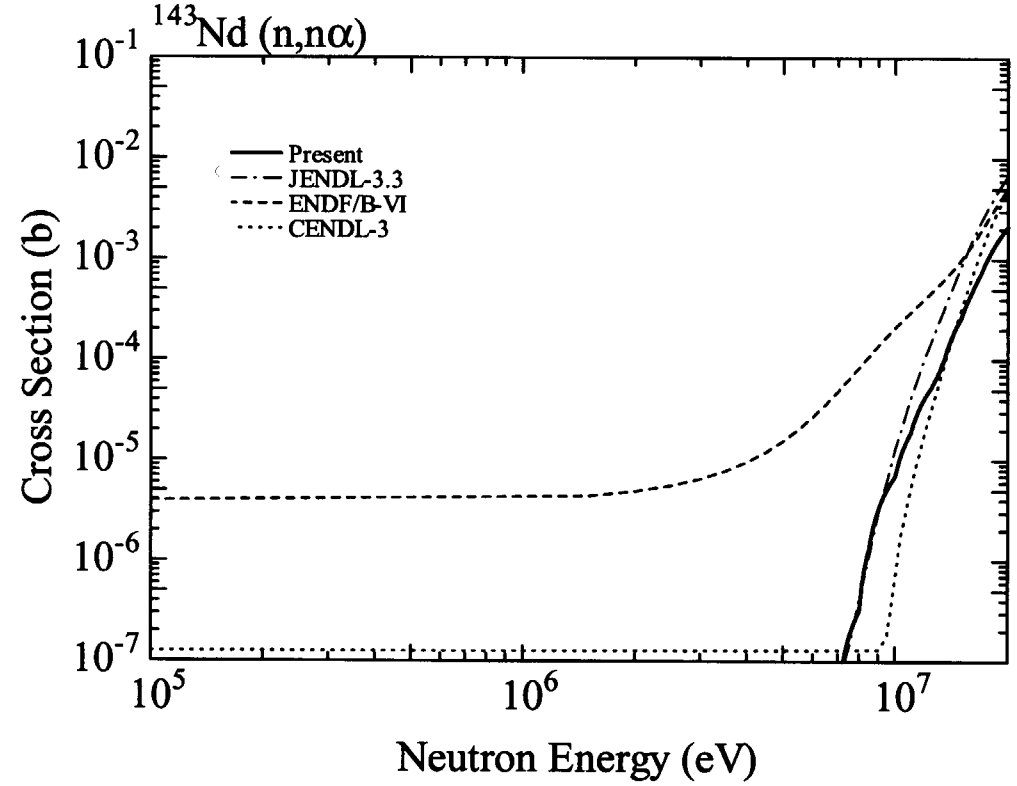

Fig. 3.16 ^{143}Nd(n,nα) reaction cross section

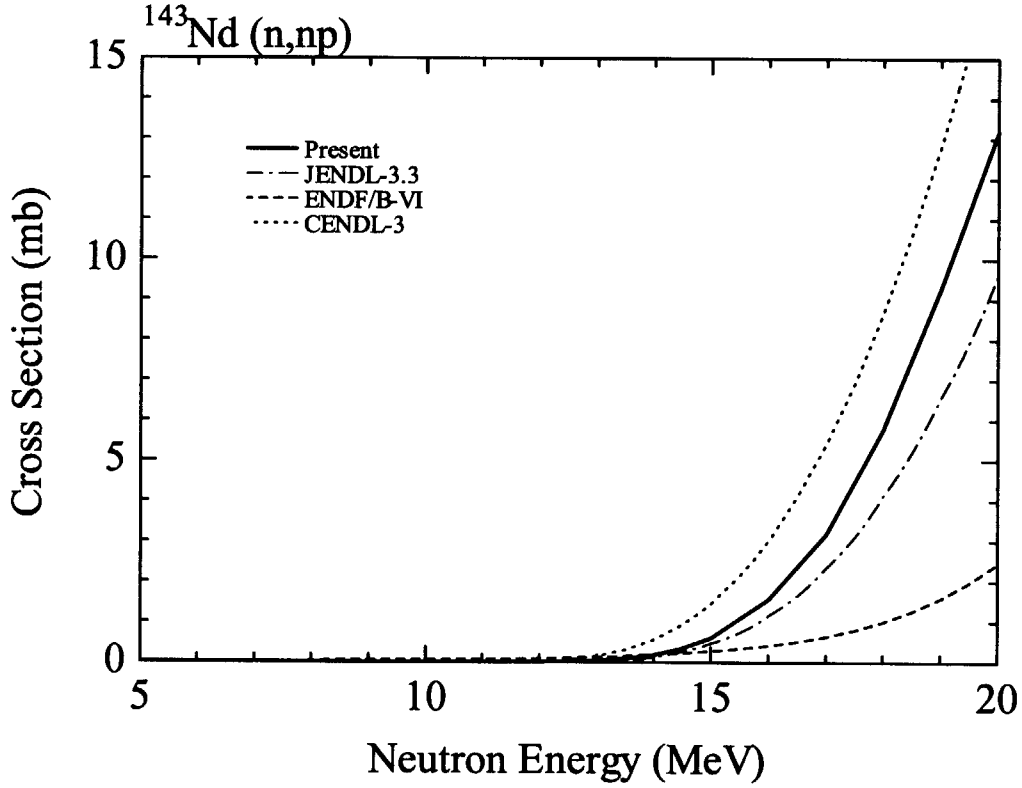

Fig. 3.17 ^{143}Nd(n,np) reaction cross section

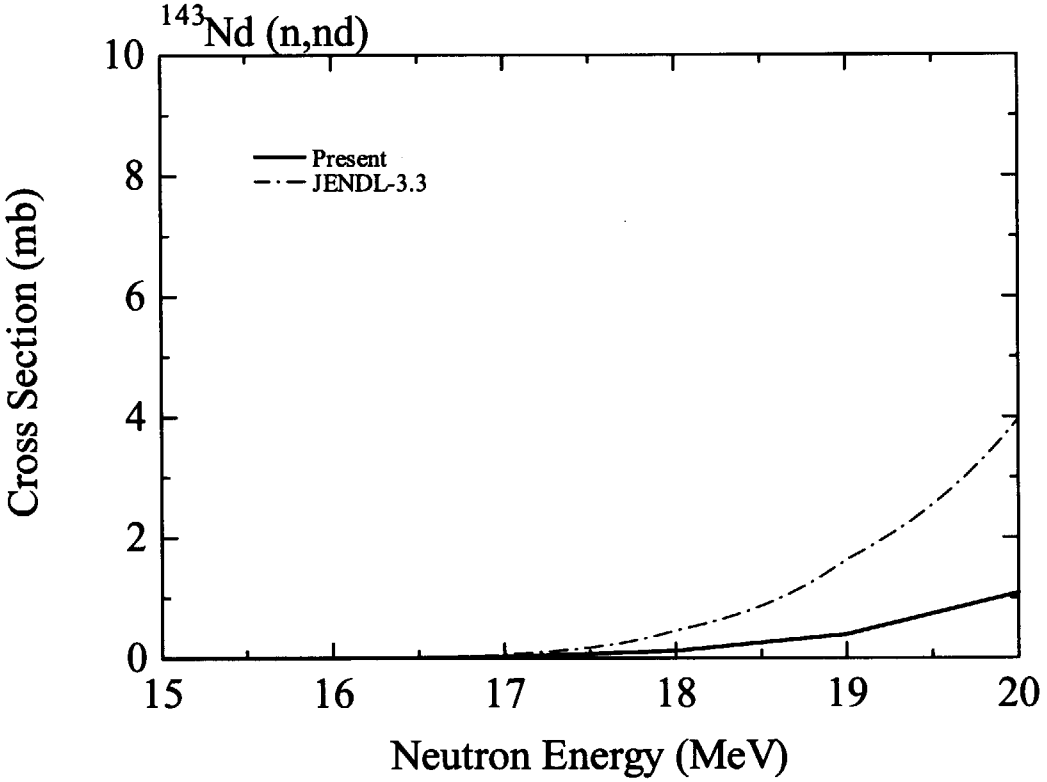

Fig. 3.18 ^{143}Nd(n,nd) reaction cross section

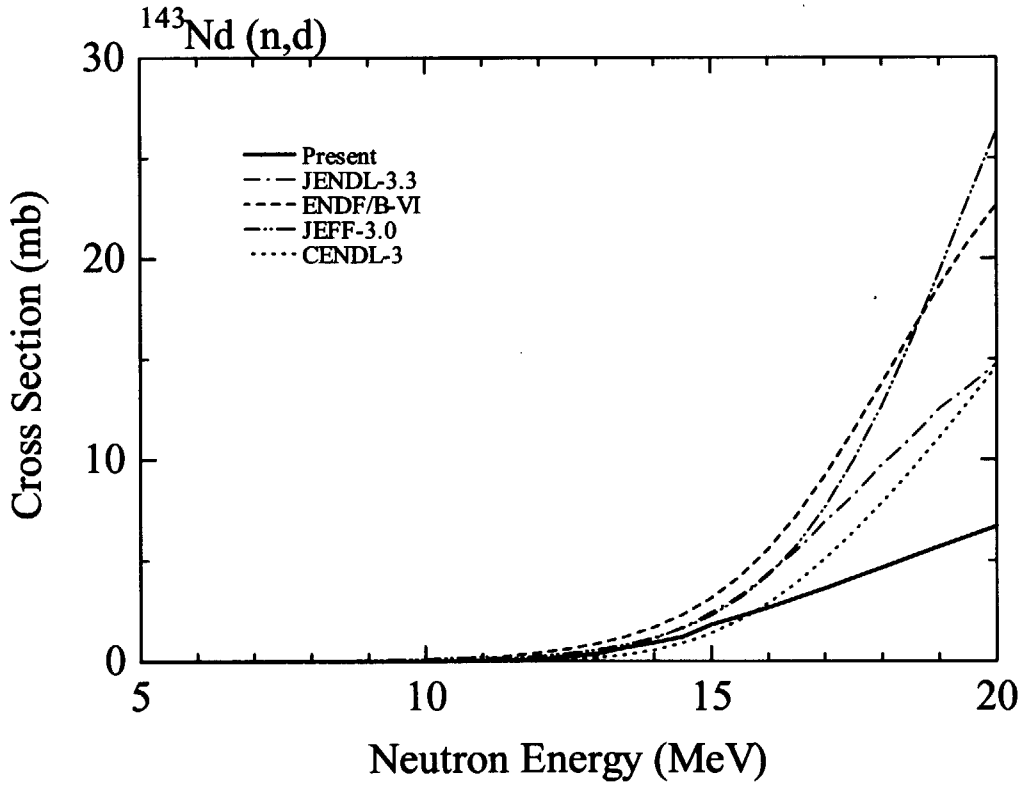

Fig. 3.19 ^{143}Nd(n,d) reaction cross section

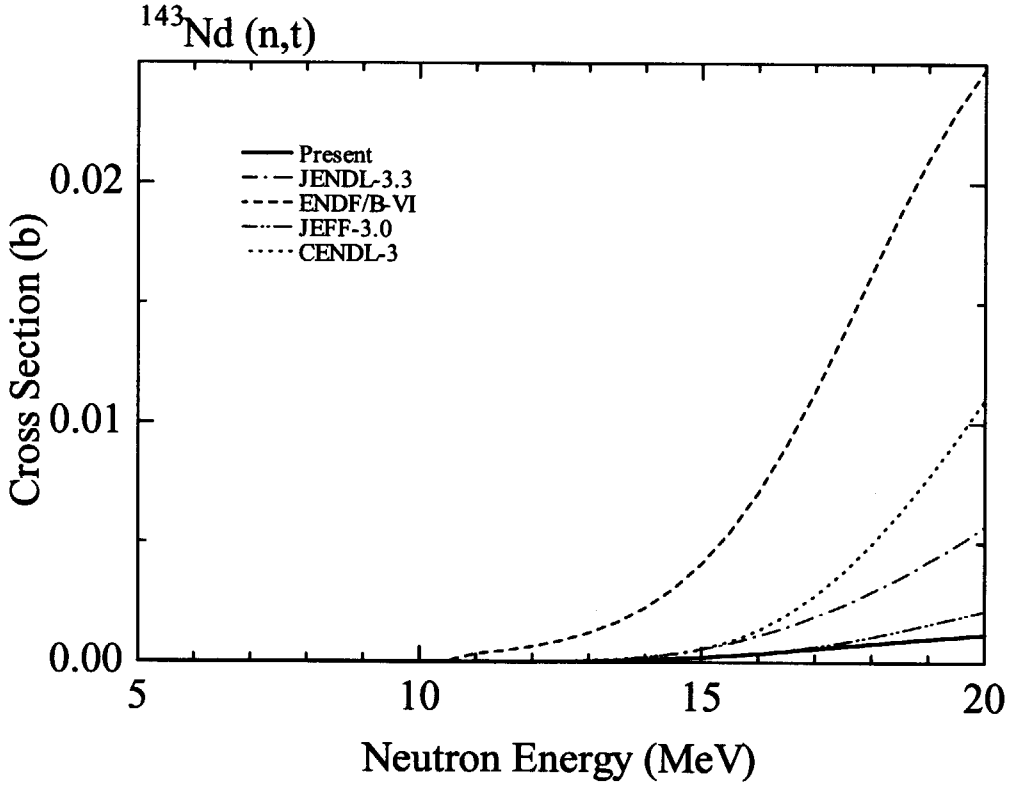

Fig. 3.20 ^{143}Nd(n,t) reaction cross section

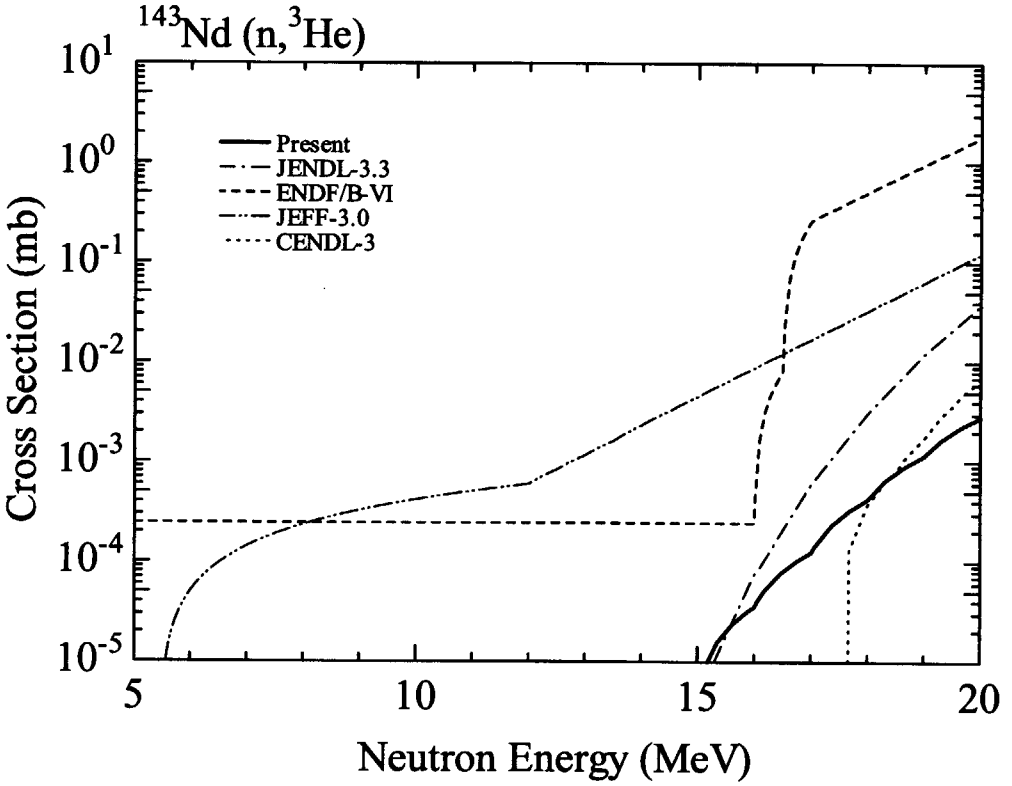

Fig. 3.21 ^{143}Nd(n,^{3}He) reaction cross section

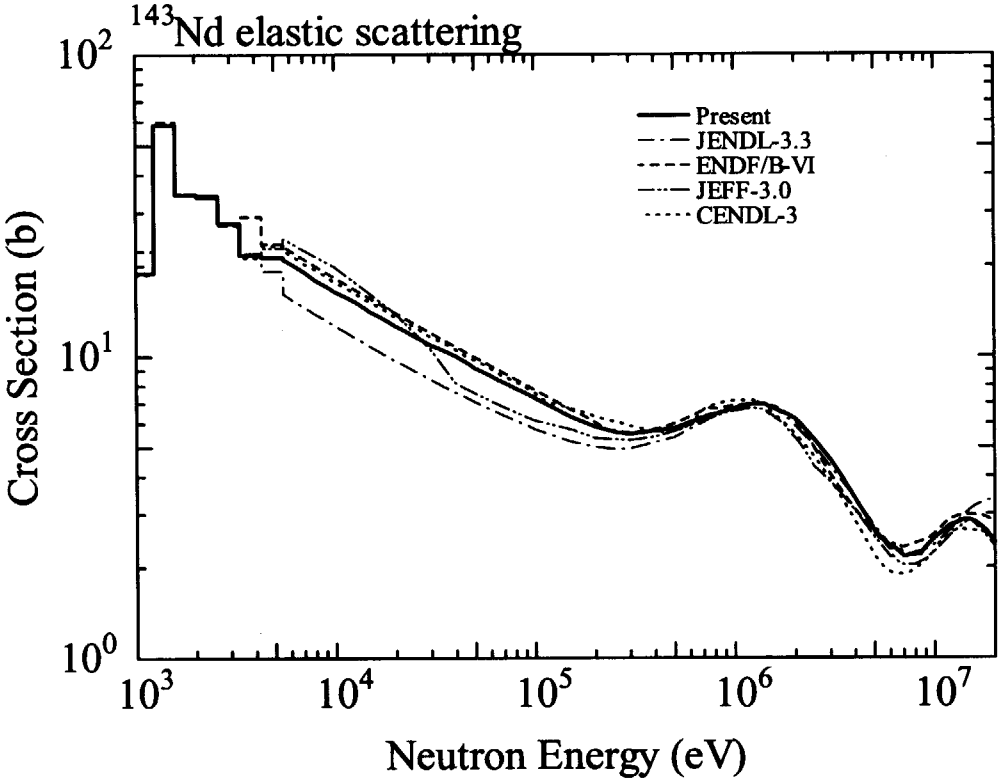

Fig. 3.22 ^{143}Nd elastic scattering cross section

国際単位系 (SI) と換算表

表 1　SI 基本単位および補助単位

量	名称	記号
長さ	メートル	m
質量	キログラム	kg
時間	秒	s
電流	アンペア	A
熱力学温度	ケルビン	K
物質量	モル	mol
光度	カンデラ	cd
平面角	ラジアン	rad
立体角	ステラジアン	sr

表 2　SI と併用される単位

名称	記号
分，時，日	min，h，d
度，分，秒	°，′，″
リットル	l，L
トン	t
電子ボルト	eV
原子質量単位	u

1 eV = 1.60218 × 10^{-19} J

1 u = 1.66054 × 10^{-27} kg

表 3　固有の名称をもつ SI 組立単位

量	名称	記号	他の SI 単位による表現
周波数	ヘルツ	Hz	s^{-1}
力	ニュートン	N	m·kg/s^2
圧力，応力	パスカル	Pa	N/m^2
エネルギー，仕事，熱量	ジュール	J	N·m
工率，放射束	ワット	W	J/s
電気量，電荷	クーロン	C	A·s
電位，電圧，起電力	ボルト	V	W/A
静電容量	ファラド	F	C/V
電気抵抗	オーム	Ω	V/A
コンダクタンス	ジーメンス	S	A/V
磁束	ウェーバ	Wb	V·s
磁束密度	テスラ	T	Wb/m^2
インダクタンス	ヘンリー	H	Wb/A
セルシウス温度	セルシウス度	℃	
光束	ルーメン	lm	cd·sr
照度	ルクス	lx	lm/m^2
放射能	ベクレル	Bq	s^{-1}
吸収線量	グレイ	Gy	J/kg
線量当量	シーベルト	Sv	J/kg

表 4　SI と共に暫定的に維持される単位

名称	記号
オングストローム	Å
バーン	b
バール	bar
ガル	Gal
キュリー	Ci
レントゲン	R
ラド	rad
レム	rem

1 Å = 0.1 nm = 10^{-10} m

1 b = 100 fm^2 = 10^{-28} m^2

1 bar = 0.1 MPa = 10^5 Pa

1 Gal = 1 cm/s^2 = 10^{-2} m/s^2

1 Ci = 3.7 × 10^{10} Bq

1 R = 2.58 × 10^{-4} C/kg

1 rad = 1 cGy = 10^{-2} Gy

1 rem = 1 cSv = 10^{-2} Sv

表 5　SI 接頭語

倍数	接頭語	記号
10^{18}	エクサ	E
10^{15}	ペタ	P
10^{12}	テラ	T
10^{9}	ギガ	G
10^{6}	メガ	M
10^{3}	キロ	k
10^{2}	ヘクト	h
10^{1}	デカ	da
10^{-1}	デシ	d
10^{-2}	センチ	c
10^{-3}	ミリ	m
10^{-6}	マイクロ	μ
10^{-9}	ナノ	n
10^{-12}	ピコ	p
10^{-15}	フェムト	f
10^{-18}	アト	a

（注）

1. 表 1 − 5 は「国際単位系」第 5 版，国際度量衡局 1985 年刊行による。ただし，1 eV および 1 u の値は CODATA の 1986 年推奨値によった。
2. 表 4 には海里，ノット，アール，ヘクタールも含まれているが日常の単位なのでここでは省略した。
3. bar は，JIS では流体の圧力を表わす場合に限り表 2 のカテゴリーに分類されている。
4. EC 閣僚理事会指令では bar，barn および「血圧の単位」mmHg を表 2 のカテゴリーに入れている。

換　算　表

力	N(=10^5 dyn)	kgf	lbf
	1	0.101972	0.224809
	9.80665	1	2.20462
	4.44822	0.453592	1

粘度　1 Pa·s(N·s/m^2) = 10 P(ポアズ)(g/(cm·s))

動粘度　1 m^2/s = 10^4 St(ストークス)(cm^2/s)

圧力	MPa(=10 bar)	kgf/cm^2	atm	mmHg(Torr)	lbf/in^2(psi)
	1	10.1972	9.86923	7.50062 × 10^3	145.038
	0.0980665	1	0.967841	735.559	14.2233
	0.101325	1.03323	1	760	14.6959
	1.33322 × 10^{-4}	1.35951 × 10^{-3}	1.31579 × 10^{-3}	1	1.93368 × 10^{-2}
	6.89476 × 10^{-3}	7.03070 × 10^{-2}	6.80460 × 10^{-2}	51.7149	1

エネルギー・仕事・熱量	J(=10^7 erg)	kgf·m	kW·h	cal(計量法)	Btu	ft·lbf	eV
	1	0.101972	2.77778 × 10^{-7}	0.238889	9.47813 × 10^{-4}	0.737562	6.24150 × 10^{18}
	9.80665	1	2.72407 × 10^{-6}	2.34270	9.29487 × 10^{-3}	7.23301	6.12082 × 10^{19}
	3.6 × 10^6	3.67098 × 10^5	1	8.59999 × 10^5	3412.13	2.65522 × 10^6	2.24694 × 10^{25}
	4.18605	0.426858	1.16279 × 10^{-6}	1	3.96759 × 10^{-3}	3.08747	2.61272 × 10^{19}
	1055.06	107.586	2.93072 × 10^{-4}	252.042	1	778.172	6.58515 × 10^{21}
	1.35582	0.138255	3.76616 × 10^{-7}	0.323890	1.28506 × 10^{-3}	1	8.46233 × 10^{18}
	1.60218 × 10^{-19}	1.63377 × 10^{-20}	4.45050 × 10^{-26}	3.82743 × 10^{-20}	1.51857 × 10^{-22}	1.18171 × 10^{-19}	1

1 cal = 4.18605 J (計量法)
= 4.184 J (熱化学)
= 4.1855 J (15 °C)
= 4.1868 J (国際蒸気表)

仕事率　1 PS (仏馬力)
= 75 kgf·m/s
= 735.499 W

放射能	Bq	Ci
	1	2.70270 × 10^{-11}
	3.7 × 10^{10}	1

吸収線量	Gy	rad
	1	100
	0.01	1

照射線量	C/kg	R
	1	3876
	2.58 × 10^{-4}	1

線量当量	Sv	rem
	1	100
	0.01	1

(86 年 12 月 26 日現在)

Re-evaluation of Neutron Nuclear Data for ^{129}I and ^{143}Nd